MICROFLUIDIC REFERENCE ELECTRODE FOR USE IN BIOFET SENSOR SYSTEMS

MICROFLUIDIC REFERENCE ELECTRODE FOR USE IN BIOFET SENSOR SYSTEMS

By

SALMAN SAFARIMOHSENABAD, B.A.Sc.

B.Sc. (Sharif University of Technology, Tehran, Iran)

A Thesis

Submitted to the School of Graduate Studies

In Partial Fulfillment of the Requirements

For the Degree

Master of Applied Science

McMaster University

Master of Applied Science (2010) McMaster University

(Mechanical Engineering) Hamilton, Ontario

TITILE:	Microfluidic Reference Electrode for Use in BioFET Sensor Systems
AUTHOR:	Salman SafariMohsenabad, B.A.Sc. (Sharif University of Technology)
SUPERVISOR(S):	Professor P. R. Selvaganapathy, Professor M. J. Deen
NUMBER OF PAGES:	Xiii, 102

Abstract

Biosensors, used in medical diagnostics, increasingly use genomic information (DNA) to rapidly and accurately determine the species present in the sample. Since, the DNA inherently has a negative charge, electrical methods provide a direct technique to sense it. This transduction has been achieved by using a biological Field-Effect-Transistor (BioFET) structure, where hybridization of a single stranded DNA (indicative of the biological species) with a complementary strand from the sample solution causes a change in the transistor characteristics that could be read out electrically. The accuracy of sensing using the BioFET is critically dependent on imposition of a highly stable potential which is performed using a reference electrode.

Design and fabrication of a miniaturized silver/silver chloride (Ag/AgCl) reference electrode is introduced in this thesis for use in BioFET. The electrode consists of Ag/AgCl wire which is embedded into a PDMS microchannel enclosed by a microcontact printed nanoporous polycarbonate membrane. The microchannel is filled with KCl solution as the internal solution.

By modifying the electrodeposition method, nanosheet AgCl structure was grown rather than the conventional globular morphology. The bare Ag/AgCl potential drift with the former morphology was found to be <0.5mV whereas the latter morphology demonstrated 2-7mV drift in 15 hours. The effect of the membrane's pore size and the internal solution on microfluidic reference electrode stability is verified, also, by using different configurations. Of them, the free-diffusion liquid junction reference electrode

with the membrane pore size of 100nm demonstrated the best performance with stability and drift of 40μV and 1mV, respectively over 100 hours. Finally, the microfluidic reference electrode was found to be insensitive to the pH and chlorine concentration of the external solution, as opposed to the bare electrode.

In conclusion, a modified electrodeposition method and free-diffusion liquid junction microfluidic reference electrode is proposed to improve the stability and extend the lifetime of a reference electrode with very low potential drift.

Acknowledgment

This section is devoted to acknowledge all kinds of assistances that I have received throughout conduction of my research in the past two years. Due to the multi-disciplinary nature of my project, the names are numerous which these few lines do not allow me to state the whole of my gratitude respect to them.

Firstly, I would like to express my appreciation to my supervisors Dr. Ravi Selvaganapathy and Dr. Jamal Deen for trusting me with this project and providing this opportunity to be involved in this project. I am also thankful for their support and guidance in entire of my project.

I would like to express my respect to Dr. Ching for his constructive comments on my project and Dr. Zhitomirsky for his valuable discussion on my results. I would also like to thank Dr. Marinov for his comments on my results throughout the thesis. The help from Waleed Shinwari on explaining the BioFET operation is warmly appreciated.

Next, many thanks to my friends in CAMEF lab, Wen, Geetha, Pouya, Mohammed, Siawash, Arash, and Simone for their help and providing a friendly work circumstance. Also, I am grateful for the support from CEDT staff Doris, Zhiling, Graham, SEM research staff Steve, and mechanical engineering technician Joe.

The last but not the least, I would like to thank my family members who inspired and supported me to continue my studies in abroad. I am in debt forever.

Table of Contents

List of Figures

List of Tables

Chapter 1

MOTIVATION AND ORGANIZATION

1.1 MOTIVATION

Early and low-cost detection of pathogens and bacteria in water and food samples is one of the important challenges of the 21st century. For instance, the World Health Organization [World Health Organization Report, 2009] reported that 88% of diarrheal deaths in the world are caused by unsafe water in 2004. About 99% of these deaths happened in developing countries and 84% of them occurred in children. Moreover, unsafe water was found to be 4th factor among 10 leading factors causing deaths in 2004 in those countries (1.6 millions, Figure 1.1).

To abate this threat, mass production of fast, low-cost, portable, and highly reliable sensors is essential to prevent spread of diseases. Various biosensors have been proposed and utilized with capability of sensing biological species using optical, mechanical, and electrical techniques [Sevilla 1994]. Recently, there has been much research interest on designing biosensors with capability of reading DNA strands. DNA is inherently negative charged molecule which indicates the unique identity of the organisms and living cells identity and carries the genomic information of them. Biosensors with capability of sensing DNA hybridization can be categorized into labelling and label-free methods. Both of them have been studied widely in the past few decades [Shinwari 2007].

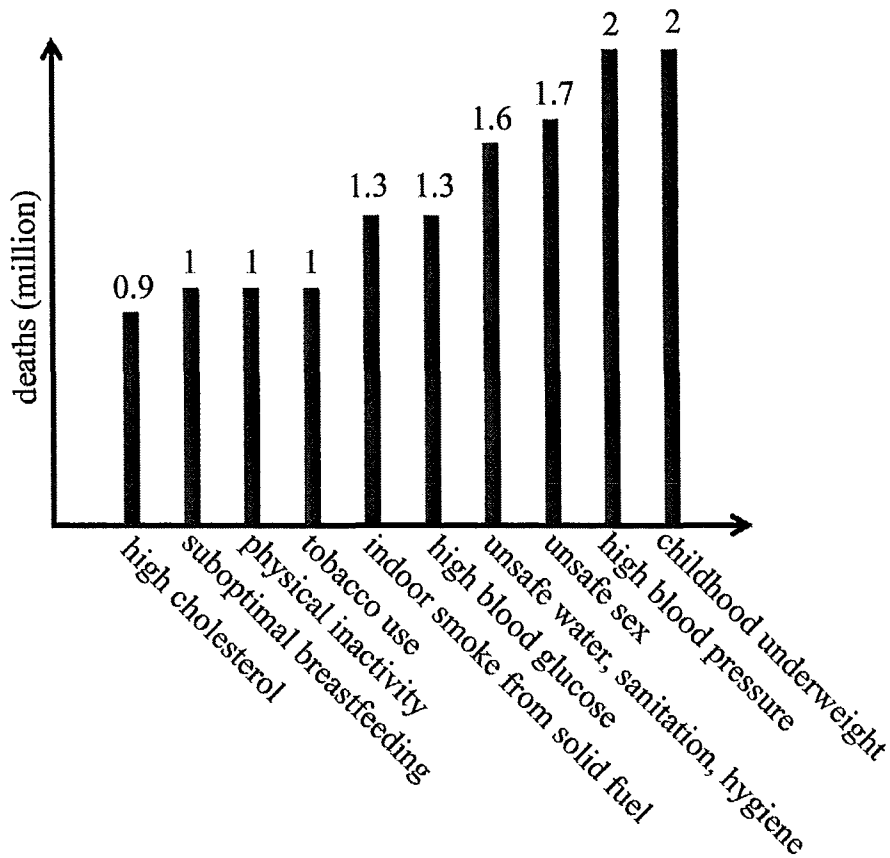

Figure 1.1 10 leading risk factor causes of death in low income counties, 2004 [World Health Organization Report, 2009].

However, the former method requires labelling tags which increases the cost and complexity of the process. Among the latter techniques, the preference is given to those which can adopt with microfabrication process and be compatible with the mainstream semiconductor technology [Shinwari 2007].

Lately, microfabricated biosensors based on Field-Effect-Transistor (FET) have been proposed to detect DNA hybridization as suitable alternatives for conventional label-free devices [Shinwari 2007]. In BioFET, metal-oxide-semiconductor (MOS) gate of the MOSFET is replaced with a solution and a reference electrode which is in contact

with the solution. In order to sense DNA hybridization, probe DNA strands are immobilized on the BioFET's gate insulator. Hybridization of the complementary DNA strands, present in the solution, with the probe DNA strands changes the transistor characteristic which can be read off electrically. Accuracy of the BioFET critically depends on the stability of the potential applied by the reference electrode at the vicinity of the gate in the solution. Hybridization of the complementary DNA strands with immobilized probe DNA strands shifts the threshold voltage several mV [Shinwari 2008]. Thereby, the stability of the reference electrode potential should be less than 1 mV to minimize its interference in the threshold voltage.

Macroscale reference electrodes have been studied since early years of 20 century [Buck 2001]. They are several types including hydrogen, calomel, silver/silver chloride, etc., that for each of them there are several modes of operation. Although macroscale reference electrode can produce stable potential for long period of operation, they are not suitable for use in BioFET that requires smaller size reference electrode. Microfabricated versions of reference electrodes have been studied extensively over the past two decades [Suzuki 1999, Simonise 2005] but they mostly suffer from fast degradation, instability, irreproducibility, sensitivity to solution analytes, and complexity of microfabrication process which make them inappropriate candidates for use in BioFETs. The objective of the thesis is outlined based on the requirements listed above for use of microscale reference electrode in BioFET.

- The fabricated reference electrode should have simple construction process and microscale sensing part (<1mm×1mm).

- It should show highly stable potential.
- It should demonstrate several hours of lifetime with the least drift.
- It should produce stable potential which is insensitive to effect of pH and chlorine concentration of external solution.

1.2 SEQUENCE OF THE CHAPTERS

The outline of the thesis is as follows:

Chapter 2 starts with introduction to biosensors, BioFET, and use of reference electrode in BioFET. It is followed by theoretical background of reference electrodes. Subsequently, types and configurations of reference electrodes are reviewed. The chapter ends with literature review of the current microfabricated reference electrodes and a brief description of their limitations for use in BioFET.

Chapter 3 deals with design and advantages of the proposed device. Also, the working principle of the designed reference electrode is explained and the possible uncertainties in the electrode potential are described.

Chapter 4 focuses on selection of the materials and microfabrication techniques used in the device fabrication. Following that, the fabrication procedure and integration of different components are explained.

Chapter 5 is devoted to the experimental setups and designs of the experiments in order to test the performance of the fabricated reference electrodes. Additionally,

experimental data and SEM pictures of the bare and microfluidic reference electrode are demonstrated in this chapter. The obtained results are discussed based on the theory introduced in chapters 2 and 3.

The contributions, made by this thesis, are listed in chapter 6. Finally, the future work and possible improvements to overcome the remaining problems are described.

Chapter 2

INTRODUCTION

2.1 BIOSENSOR

Biosensors are devices that are capable of detection of biological materials including proteins [Koch 1999], neurons [Martinoia 2004], cells [Offenhausser 2001], and microorganism [Schöning 2002]. Of these, DNA biosensors are increasingly used as medical diagnostic tools due to their ability to identify specific sequence of DNA. DNA carries the genomic information of its host cell [Stryer 1995] and can be regarded as a unique indication of its host cell. Furthermore, it has negative charge naturally and therefore can be sensed electrically.

Biosensors consist of two parts including sensing element and transducer. DNA biosensors can be categorized based on their sensing process into hybridization, amplification, and separation based series [Selvaganapathy 2003]. For example in a hybridization based biosensor, DNA strands of known pathogens can be extracted, and amplified using PCR (polymerase chain reaction) method [Gabig 2001], and functionalized as probe DNA on the biosensor. If probe and target strands (introduced from the sample DNA) match each other, hybridization process occurs which can be sensed by the biosensor. The second classification of the biosensors can be performed based on the types of the transducers which are used to read the DNA molecules. It includes optical [Heller 2002], mechanical [Okahata 1992, Bashir 2004] and electrical sensors [Long 2003, Hleli 2003, Shinwari 2006]. Example of the optical sensors can be

found in DNA microarray devices. They consist of hundreds of microreservoirs on which the probe DNA strands are immobilized [Heller 2002]. Following the probe DNA immobilization, the target DNA strands are labelled by fluorescent agents and introduced to the microreservoirs. After the hybridization, the microarray is scanned under laser scanner and the intensity of the emitted light is considered as an index of the density of the hybridized DNA molecules. The image signature of the microarray can be analyzed using image processing technique to determine the nature of the target DNA strands. This technique has excellent merits due to its sensitivity, however, use of labelling agents and precise scanner increases its cost.

Mechanical sensors can be also categorized into piezoelectric and piezoresistive sensors. For instance, in quartz crystal microbalance sensor [Okahata 1992] the probe DNA strands are immobilized on a crystal's surface. Once the hybridization between the probe and target DNA strands occurs the oscillation frequency of the crystal decreases due to the mass increment of the crystal. Finally, electrical based biosensors can be classified into capacitive, resistive, and Field-Effect-Transistor (FET) based sensors. For example, AC impedance spectroscopy method can be used to detect hybridization of the DNA strands in an electrochemical cell [Wilson 2001]. If the probe DNA is immobilized on the electrode of the electrochemical cell, hybridization of the target DNA strands will result in impedance (capacitance) changes to this interface. This change has been attributed to the conductive properties of the DNA by some researchers [Long 2003], while others relate it to the effects which the DNA molecules have on the interfacial capacitance [Hleli 2003].

Over the few past decades, microfabrication methods have been used to reduce the fabrication cost and power consumption of these sensors. Electrical sensors based on FET phenomenon are one of the most desirable miniaturized sensors since they can be easily adapted to the microfabrication process. For example, Ion-Sensitive-Field-Effect-Transistor (ISFET) structures were introduced by [Bergveld 1970] and were used as pH sensors. It is a modified version of Metal-Oxide-Semiconductor-Field-Effect-Transistor (MOSFET) in which gate of the MOSFET is replaced with a solution and a reference electrode that is immersed in the solution. Another example is Electrolyte-Insulator-Semiconductor-Field-Effect-Transistor (EISFET) which is similar to ISFET in terms of structure. The main purpose of this structure is to enable interaction of the electrolyte with the electronic substrate. Such a structure can allow electronic sensing of chemical and biological material that become immobilized on the surface [Shinwari 2006].

A very recent version of FET sensor is BioFET which is capable of in-situ identification of the DNA sequence [Sevilla 1994, Shinwari 2007]. It is a modified version of MOSFET in which gate and polysilicon are removed and the underlying dielectric is functionalized chemically. The dielectric is in contact with a solution and a reference electrode that is immersed in the solution. This type of sensors has several advantages over the previously fabricated biosensors. First and most important of all, it provides a direct method of label-free electrical detection of DNA hybridization using cheap complementary metal-oxide-semiconductor (CMOS) silicon technology. In addition, the continued miniaturization of CMOS allows detection in dilute sample solution due to the smaller sensing bio-active surface [Shinwari 2007]. Also, the BioFET

array can be easily integrated with the accompanying electronics for signal processing on the same chip. DNA microarrays, which are built this way, would be ideal candidates for a portable DNA analysis and pathogen detection device.

2.2 BIOFET

The BioFET, as shown in Figure 2.1, can be described as a Field-Effect-Transistor whose gate has been replaced with a solution and reference electrode and the dielectric has been chemically functionalized. The sensor has a semiconductor substrate that is doped with boron (p-type). It has two regions close to the surface, which are doped with phosphorous (n-type), that serve as source and drain terminals. By imposing potential through the reference electrode in the solution close to the gate dielectric, counter charges can be accumulated or depleted in the semiconductor. If enough electric field is imposed through the reference electrode, accumulation of counter charge can be sufficient to create a channel between the source and drain. It can flow if potential difference exists between terminals (see Figure 2.1).

DNA of known pathogens can be synthesized and functionalized chemically at their tails and spotted on the dielectric material as probe strands. To apply potential to BioFET, a liquid medium (typically phosphate buffer saline (PBS)), is used. When complementary DNA is present in the sample solution, it hybridizes with the probe DNA attached onto the gate insulator and effectively doubles the charge at the gate. Since the sample DNA is present in the solution; the gate bias, which is needed to be applied to create the underlying channel, should increase.

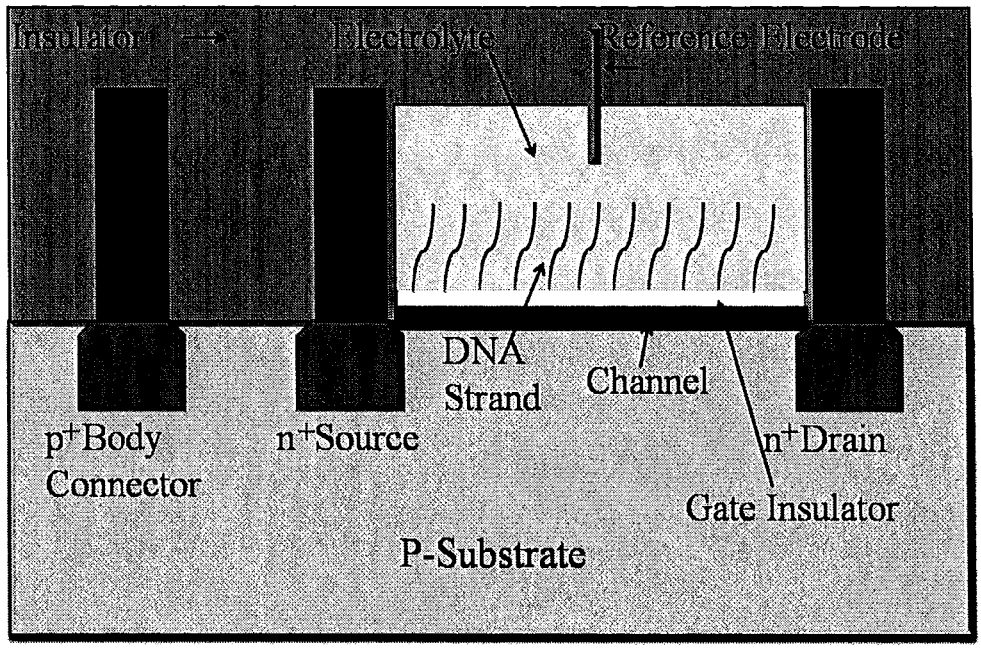

Figure 2.1 Schematic diagram of BioFET.

The threshold voltage to create the aforementioned channel is higher with respect to the case in which there is no hybridization. For example, [Sakata 2005] reported variation of 11 mV in the threshold voltage due to the hybridization of 100 μM target DNA (density of $1.7\times10^{8}/cm^{2}$) within 12 hours in a phosphate buffer solution.

The main parameter that determines the sensitivity of the BioFET is the amount of DNA probes that attract target molecules and produce an electrical signal [Shinwari 2007]. As density of it decreases the stability of the threshold potential which is applied through the reference electrode should be higher. In fact, shift in the threshold voltage is sum of several components including the reference electrode potential, affinity of the solution, affinity of the Silicon [Shinwari 2008]. All factors contributing to the threshold voltage can be minimized sufficiently during the fabrication process except for

the reference electrode potential. In order to retain the high accuracy, the primary requirement for a reference electrode is to maintain its potential stability as much as possible, significantly lower than 1 mV during its operation. In addition, the BioFET is in array format which allows multiple operation of the BioFET by using part of the array each time. Therefore, another criterion for the reference electrode is long lifetime so that it is reusable for long period of time. Also, multi-use BioFET needs replacement of the electrolyte for each run so that it requires a reference electrode insensitive to the analytes presenting in the test media. In addition, the reference electrode should be integrated on the BioFET reservoir in such a way that its potential imposition panel is in contact with the solution. Structure of the BioFET array dictates use of a miniaturized planar reference electrode to fit the reservoir of the BioFET chip (see Figure 2.1).

2.3 REFERENCE ELECTRODE

2.3.1 INTRODUCTION

Reference electrodes are well-known for their applications in electrochemical sensors where potential is to be sensed in a solution. Their applications include area such as analytical measurements [Severinghaus 1958], electroplating [Amadi 1991], electroencephalography [Niedermeyer 2005], and corrosion [Wolfe 2005]. Conventional examples of electrochemical sensors are pH meter and gas sensors which can be used to detect pH in the solutions and polluting gases in air, respectively [Bakker 2002, Guth 2009]. The typical electrochemical sensor consists of a reference electrode and working electrode (see Figure 2.2). The former is absolutely insensitive to

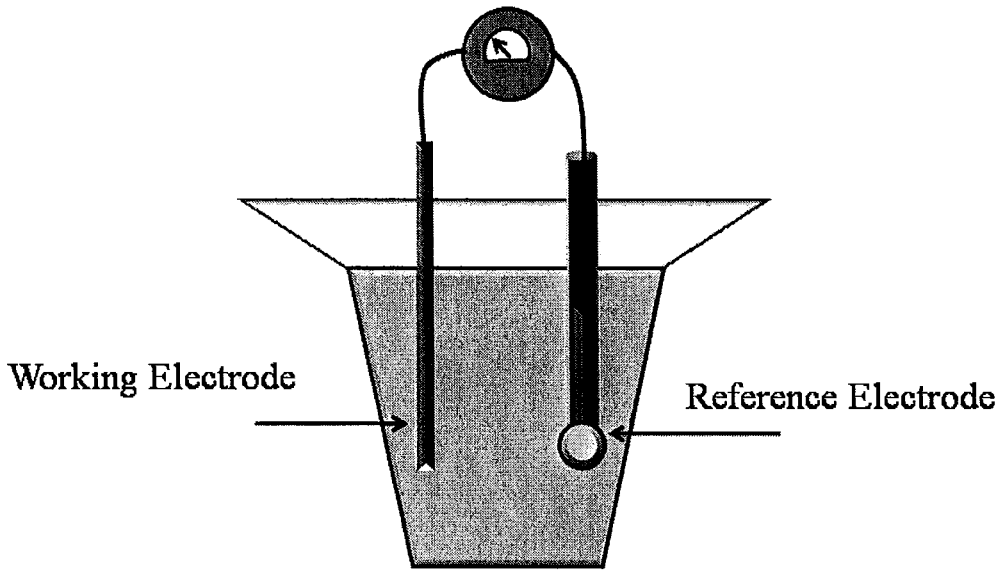

Figure 2.2 Schematic of an electrochemical sensor.

the analytes inside the test medium and can maintain its electrochemical potential stable whereas the latter is highly sensitive to certain analytes. Based on the following relation which is termed Nernst response, the electrochemical potential of the electrode can be estimated:

$$E=E^{\circ}-(RT/ZF)\ln(K) \quad (2.1)$$

where E is the equilibrium potential, E° is the standard reduction potential of the electrode against the standard hydrogen electrode, R is the universal gas constant, T is the temperature in Kelvin, Z is the number of electrons transferred, F is Faraday's constant and K denotes reaction coefficient. The working electrode electrochemical potential depends on the concentration of the analytes participating in the reaction and their valences (see section 2.3.2 for more details). Accordingly, concentration of the ion or analyte of interest in the solution can be correlated by measuring the potential difference

between the working and reference electrodes. Thereby, reference electrode potential stability has a critical impact on electrochemical sensor accuracy.

Reference electrodes can be used in conjunction with sensing tools in many biosensing applications such as ISFET [Smith 1986, Wong 1989] where a reference electrode is used to impose an electric field across the electrolyte unit of the sensor to detect residues inside the electrolyte. Also, reference electrode applications can be found in sensing of bioimpedance of the stratum corneum [Benjamin 2005] and biosensors such as glucose sensor [Zhang 1999], lactose sensor [Sevilla 1994], albumin detection [Park 2008], and DNA sequence detection [Sakata 2005, Shinwari 2007].

2.3.2 THEORY

(I) Concept of Electrode Potential

In galvanic cell, the electrochemical potential of charges can be defined based on the Gibbs free energy variation which comprises of different processes. Each of them involves transferring of ions and electrons in which there is a specific energy transfer which makes different galvanic potential [Ives 1961]. A suitable approach to obtain the electrochemical potential can be relating the free energy to the chemical potential of the ions assuming that their chemical potential is uniform throughout the system. The definition of the chemical potential is as follows [Ives 1961]:

$$\mu_i=(\partial G/\partial n_i)_{T,P,n_j} \tag{2.2}$$

where μ_i is the chemical potential, G is Gibbs free energy, n_i is molarities of component i, n_j is molarities of component j, T and P stand for temperature and pressure, respectively.

Since ions in solution are always electro-neutral, equation (2.2) can be used to define the free energy in terms of the constituent chemical potential of ions [Ives 1961]:

$$dG = (\partial G/\partial n_i)_{T,P,n_j} dn_i + (\partial G/\partial n_j)_{T,P,n_i} dn_j = \mu_i dn_i + \mu_j dn_j \quad (2.3)$$

For instance, the chemical potential of potassium chloride in aqueous solution is a combination of potassium ions and chlorine chemical potentials. The change in the free energy can be related to the electrochemical potential through the following equation [Ives 1961]:

$$nFE = -\Delta G \quad (2.4)$$

where n is the number of electron transferred, F is Faraday's constant, E is the equilibrium potential. It is possible to measure the electrochemical potential between two cells considering a galvanic cell which derives the electrical energy from a chemical reaction. The following reaction mimics the actual reactions which happen in galvanic cells:

$$AB(s) + e^- \leftrightarrow A(aq) + B(aq) \quad (2.5)$$

In open-circuit potential test, the system is in balance and the forward and backward reactions occur at the same rate and overall reaction is in equilibrium. At certain temperature, if all the reactants are at their standard states, the free energy change and electromotive force of the cell reaction will be the same as their standard values, ΔG° and E°. The chemical potential of a specie can be related to its activity by the following relationship:

$$\mu_i = \mu_i^\circ + RT \ln(a_i/a_i^\circ) \quad (2.6)$$

where R is the gas constant per mole, T is the absolute temperature, a_i is the component i activity at the state which its chemical potential is μ_i, a_i° is the component i standard activity at the standard state which its standard chemical potential is μ_i°. The value of a_i° is unity. For gases the activity can be replaced with pressure. Likewise, for aqueous solutions activity of ions can be represented by their concentration. Therefore in reaction (2.5) [Ives 1961]:

$$\Delta G = \mu_A^{solution} + \mu_B^{solution} \tag{2.7}$$

Note the activity of the substances in solid state is not accounted. When a solid material dissolves, only soluble products contribution is accounted to determine reaction activity [Ives 1961]. By combining equation (2.7) into equation (2.6):

$$\Delta G = \mu_A^\circ + RT \ln(a_A/a_A^\circ) + \mu_B^\circ + RT \ln(a_B/a_B^\circ) \tag{2.8}$$

$$\Delta G = \Delta G^\circ + RT \ln(a_A) + RT \ln(a_B) \tag{2.9}$$

From equation (2.4), equation (2.9) becomes:

$$nFE = nFE^\circ + RT \ln(a_A) + RT \ln(a_B) \tag{2.10}$$

Dividing both sides of equation (2.10) by nF, the following equation is obtained:

$$E = E^\circ + (RT/nF) \ln(a_A) + (RT/nF) \ln(a_B) \tag{2.11}$$

where E° is the standard electrochemical potential. E° of the standard hydrogen electrode (SHE) is set to be zero and the standard potential of all other electrode reactions are obtained with reference to SHE. Equation (2.11) is termed Nernst response which is one of the fundamental relationships in electrochemistry.

(II) Current-Voltage Characteristics

The relationship between the applied potential and the resulting current in an electrochemical system depends on the electrode/electrolyte interface. When the applied overpotential η (=E- E°) is low, the concentration of reactants at the electrode/electrolyte interface is not exhausted and the reaction is said to be kinetically controlled. In this case, the current has an exponential relationship with the applied overpotential η (=E- E°) as proposed by Tafel in 1905 [Bard 1980]:

$$\eta = a' + b' \log I \tag{2.12}$$

where I is the current, a' and b' are empirically determinable coefficients. Let us consider that the forward path of reaction (2.5) occurs at rate of υ_f that is proportional to the surface concentration of oxidants. The concentration of oxidants at distance x from the surface and at the surface at time t is $C_o(x,t)$ and $C_o(0,t)$, respectively [Bard 1980]:

$$\upsilon_f = K^{\circ} e^{-\alpha nF(E-E^{\circ})/RT} C_o(0,t) = \frac{I_c}{nFA} \tag{2.13}$$

$K^{\circ}$and α are the standard rate constant and the transfer coefficient, respectively which are adjustable, I_c is the cathodic current, and A is the reacting surface area. Similarly for reverse reaction, the following relationship exists for reductants:

$$\upsilon_b = K^{\circ} e^{(1-\alpha)nF(E-E^{\circ})/RT} C_R(0,t) = \frac{I_a}{nFA} \tag{2.14}$$

where I_b denotes the anodic current density. Thus, the overall current, which flows within the system, is as follows:

$$\upsilon_{net} = \upsilon_f - \upsilon_b = \frac{I_c - I_a}{nFA} = \frac{I}{nFA} \tag{2.15}$$

The current density can be calculated using the below relation:

$$j = I / A = nFK^{\circ}\left[C_o(0,t)e^{-\alpha nF(E-E^{\circ})/RT} - C_R(0,t)e^{(1-\alpha)nF(E-E^{\circ})/RT}\right] \quad (2.16)$$

From 2.3.2 (I), we know that activity of an aqueous solution can be represented by concentration of analytes. As a result, equation (2.11) can be written as follows:

$$(E\text{-}E^{\circ})(nF)/(RT) = \ln(C_o) + \ln(C_R) \quad (2.17)$$

At equilibrium condition, concentrations of oxidants and reductants in the bulk and at the electrode surface are the same, respectively. By substituting equation (2.17) into equation (2.16) and for the particular case C_o=C_R=C:

$$j_{\circ} = I_{\circ} / A = nFK^{\circ}C \quad (2.18)$$

$j_{\circ}$ is called exchange current density. Although the net current is zero in equilibrium state, the exchange current density represents balanced Faradaic activity. The higher exchange current density results in faster electron transfer in electrode/electrolyte interface which results in electrode with more stable potential. Finally, equation (2.16) becomes simplified as follows:

$$j = j_{\circ}\left[e^{-\alpha nF(E-E^{\circ})/RT} - e^{(1-\alpha)nF(E-E^{\circ})/RT}\right] \quad (2.19)$$

Once electrode surface is in contact with solution, electrochemical reactions happen because of the difference in electrochemical potentials. If no energy is introduced to the system, it is in equilibrium state (see Figure 2.3). If the electrode is tested versus the standard hydrogen electrode, the potential is E° which represents the potential difference between reactants and products at standard non-equilibrium condition. When an external energy source is introduced to the system, the electrode potential changes from E° to E. When a low overpotential is applied to the system, the reaction barrier

determines the rate of conversion of reactants into products. In this case, current can be obtained using equation (2.19). Applying high overpotential leads the reaction towards mass transport condition. In this case, due to the fast depletion of reactants, mass transport from the bulk to the surface becomes significant. The rate of reaction is then determined by contribution of diffusion, conduction and convection. Diffusion occurs once concentration gradient is built up between bulk solution and electrode surface. Conduction of charges happens in presence of external electric field. If solution is stirred, the flow of solution can drag some of the charges in bulk solution to electrode surface.

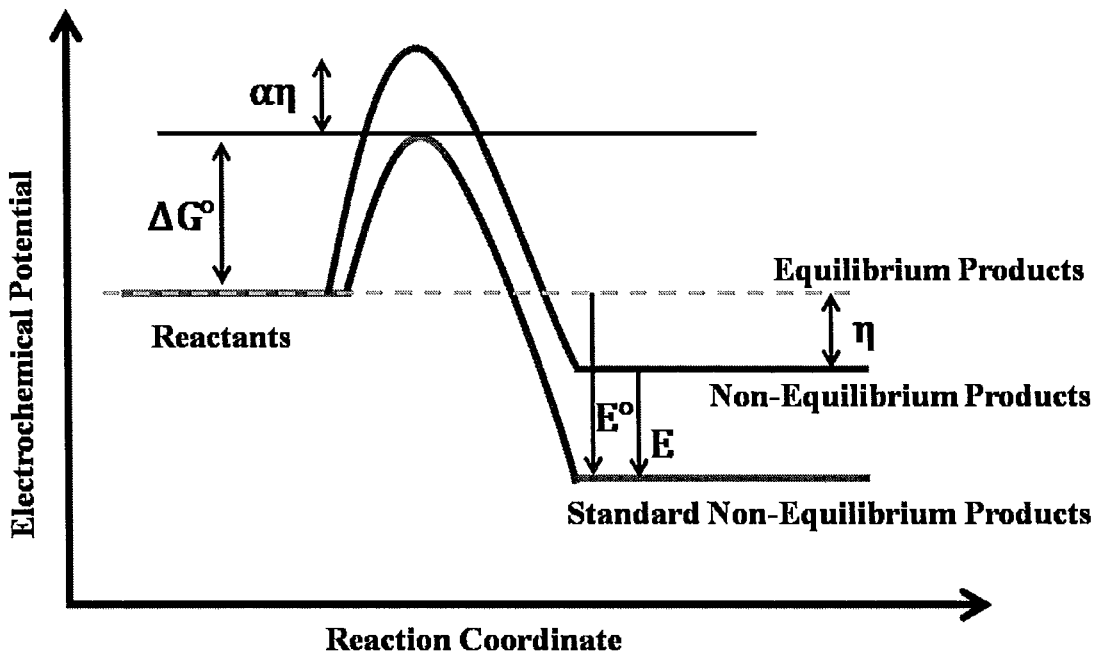

Figure 2.3 Effect of over potential on reaction potential.

(III) Non-Steady State Mass Transport Mode

Applying high overpotential drives the reaction towards mass transport condition in which equation (2.19) is not applicable any more. In the absence of convection, the current can be related to concentration gradient by the following relation (for more details refer to [Bard 1980]):

$$D\left(\frac{\partial C}{\partial z}\right)_{z=0} = \frac{I}{nFA} \tag{2.20}$$

where z indicates the distance from the electrode surface. In case when convection is present, a stagnant layer δ is established at electrode surface in which diffusion maintains the mass transfer. Outside of this layer, convection maintains the mass transfer rate. Stagnant layer thickness can be defined by the following equation [Bard 1980]:

$$\delta(t) = 2\sqrt{Dt} \tag{2.21}$$

δ is the stagnant layer thickness of the produced layer, D is diffusion coefficient, and t is elapsed deposition time. The corresponding concentration gradient is as follows:

$$\left(\frac{\partial C}{\partial z}\right)_{0\leq z\leq\delta} = \frac{C^* - C(z=0)}{\delta} \tag{2.22}$$

where C^* is the concentration of ion of interest in the bulk solution. Accordingly, equation (2.20) becomes:

$$\frac{I}{nFA} = \frac{D^{1/2}}{2t^{1/2}}[C^* - C(z=0)] \tag{2.23}$$

2.3.3 REFERENCE ELECTRODES: TYPES & THEIR MINIATURIZATION

Reference electrodes can be classified based on their electrode reactions:

(I) Standard Hydrogen Electrode

It consists of a platinum surface (noble metal) blanketed by a layer of black platinum (Figure 2.4). Black platinum plays the role of catalyst for reduction of protonated hydrogen. Platinum is in contact with an acidic solution enclosed by glass chamber in which hydrogen pressure is kept constant (Figure 2.4).

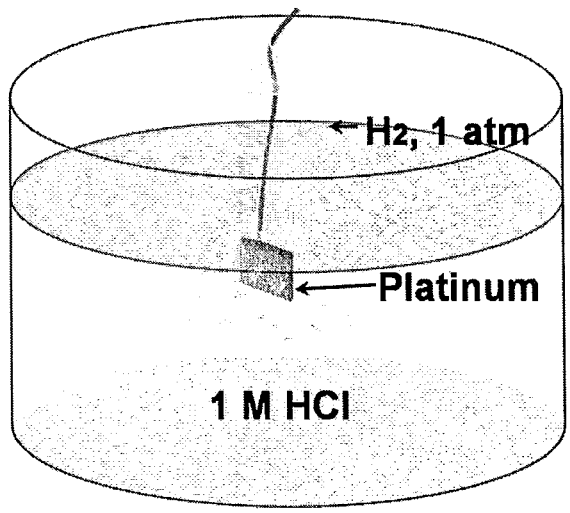

Figure 2.4 Standard hydrogen electrode.

Since metal is in direct contact with the solution and there is no participation of platinum salt in electrode reaction, it is called electrode of the first kind [Ives 1961]. The hydrogen electrode is also known as an oxidation-reduction electrode in which equilibrium is established between hydrogen ions in the solution, platinum and absorbed hydrogen

molecules in the metal. Bubble generation at the electrode surface is visible once reduction process progresses based on the following reaction:

$$2H^{+}(aq) + 2e^{-} \leftrightarrow H_2(g) \quad (2.24)$$

Thus, the electrochemical potential of the electrode can be represented by substituting the reaction properties in equation (2.11):

$$E=(RT/2F)\ln(C_{H^+})^2 - (RT/2F)\ln(P_{H_2}) \quad (2.25)$$

Equation (2.25) illustrates effect of hydrogen ion concentration and hydrogen pressure on electrode electrochemical potential. As mentioned earlier, hydrogen pressure is kept constant and normally 1 atm. Therefore, the hydrogen concentration solely affects the potential. Hydrogen electrode has high exchange current density making it a favourite probe for study of acidic, basic, and buffer solutions [Ives 1961, Shinwari 2010]. Hydrogen electrode is one of the most important reference electrodes that its electrochemical potential is presumed zero and other reference electrodes potential are measured with respect to it.

The first attempts for miniaturization of hydrogen electrode can be referred back to early 20st century [Salle 1929] in which platinum wire was sealed into a tube with millimetre dimension. It was used to determine hydrogen concentration in blood and other biological fluids with contact area of several mm^2. Several decades later, [Bard 1962] made a hydrogen electrode in which platinum wire with diameter of 510 μm was coiled. He showed that the rate of hydrogen ion reduction in acidic halide media decreased at a platinum electrode in the presence of tin. In another design, Pt wire with diameter of 1 mm immersed in a tube which was filled with a thin film of electrolyte

which allowed rapid diffusion of hydrogen at electrode surface [Will 1986]. Stability was found to be 0.5 mV over the time period of several days. [Duan 2001] used electrochemical etching process to create a highly porous columnar thin layer of Pt on the electrode surface. The fabricated reference electrode was shown to be implementable in biosensors to detect the electrical characteristics of living biological materials. Novel microtubular hydrogen electrode fabrication process was reported by [Kunimatsu 2005]. Black platinum catalyst paste was injected into the tubes which contained Pt wire and perfluorosulfonic acid polymer as electrolyte. The fabricated electrode showed stability of ±0.2 mV in sulphuric acid in about 5 min.

Dynamic reference hydrogen electrode is another approach to miniaturization [Giner 1964, Nann 2000]. In this configuration [Giner 1964], a constant current density of 1 mA/cm^2 is drawn between two platinised platinum electrode placed close to each other in an acid or alkaline medium which results in generation of H_2 gas at the cathode and O_2 at the anode. Stability of 5 mV over 5 days was obtained using this configuration [Giner 1964]. A protective polymeric membrane of polyhydroxyethylmethacrylate hydrogel was used by [Nann 2000] in the same configuration as explained above to provide potential stability to varying flows [Nann 2000].

(II) Calomel Reference Electrode

It consists of mercury metal with a layer of calomel (mercury chloride) (Figure 2.5). The electrode is in contact with saturated KCl encapsulated in a glass chamber. Glass chamber has a porous interface which acts as a liquid junction between

internal and external solutions (Figure 2.5). They are some pronounced advantages associated with this electrode including ease of construction, high exchange current density and non-polarisablity. It is known as electrode of the second kind due to participation of mercurous salt at electrode electrochemical reaction. The electrochemical reaction occurs as follows:

$$Hg_2Cl_2(s) + 2e^- \leftrightarrow 2Hg(l) + 2Cl^-(aq) \quad (2.26)$$

Exchange current density of this reaction has been found to be 1 A/cm^2 [Bockris 1964]. The electrode potential can be obtained by the following equation:

$$E=E^{\circ}_{Hg_2Cl_2} - (RT/F)\ln(C_{Cl^-}) \quad (2.27)$$

Equation (2.27) depicts the predominant effect of chlorine concentration on electrode potential. $E^{\circ}_{Hg_2Cl_2}$ is 245mV versus standard hydrogen electrode.

There are very few research works devoted to miniaturized calomel electrode due to hazards associated with mercury storage and handling process. A miniaturized calomel electrode was introduced and used by [Shibata 1977] to record DC potential variation in freely moving rats.

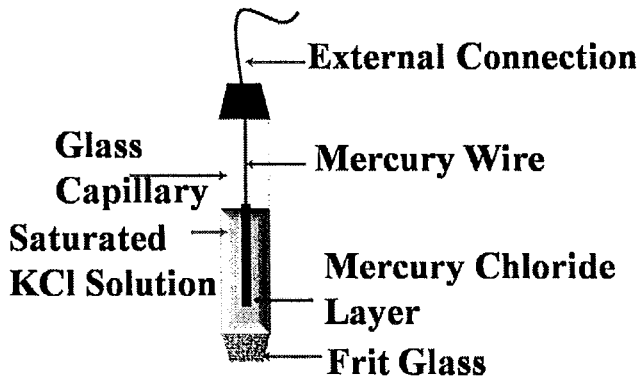

Figure 2.5 Calomel reference electrode.

It consisted of a glass capillary pipette with a mixture of saline and agar as junction, separated from mercury by a layer of calomel (Hg_2Cl_2) and cotton with Pt wire as external connection. It showed 11.4 mV drift during 5 weeks of operation.

In another work, calomel reference electrode based on the non-toxic silver solid amalgam (SCE-AgSA) was used as an alternative for liquid mercury [Yosypchuk 2003]. Stable electrode potential with fluctuation of ±1 mV in saturated KCl was reported by them during one week of operation.

(III) Silver/Silver Chloride Reference Electrode

One of the well-known types of reference electrodes is silver/silver chloride electrode in contact with saturated KCl. It is a non-polarisable electrode which has high exchange current density (1 A/cm^2 [Roberge 2000]). It is known as electrode of the second kind due to participation of silver salt in the electrochemical reaction.

$$AgCl(s) + e^- \leftrightarrow Ag(s) + Cl^-(aq) \tag{2.28}$$

The electrochemical potential for silver/silver chloride can be obtained by:

$$E = E^{\circ}_{AgCl} - (RT/F) \ln C_{Cl^-} \tag{2.29}$$

where its standard electrode potential equals to 197 mV versus the standard hydrogen electrode. Based on equation (2.29) chlorine concentration is expected to have the main impact on the electrode potential. The typical macroscale Ag/AgCl electrode comes in different configurations. The simplest reference electrode is silver wire which has been converted into silver chloride partially [Kulys 1994] (Figure 2.6 (a)). This configuration is termed quasi-solid-state reference electrode. Although the fabrication is simple, this

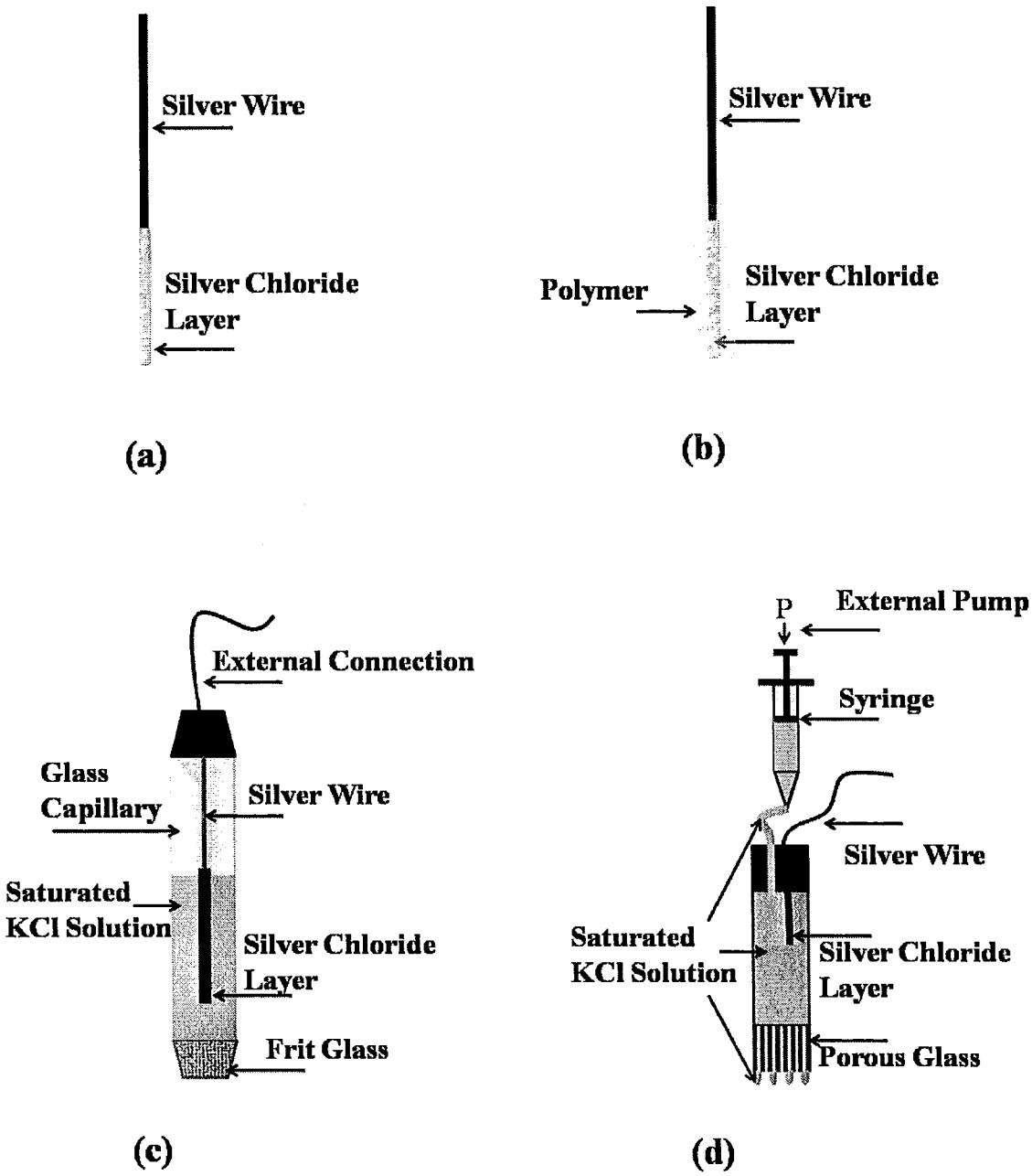

Figure 2.6 Different configurations of silver/silver chloride reference electrode (a) quasi-solid-state reference electrode (b) solid-state reference electrode (c) liquid junction reference electrode (d) free-diffusion liquid junction reference electrode.

kind of electrode suffers from high instability with variation in test solution conditions. The instability is attributed to the effect of the test solution chlorine concentration since the electrode is in direct contact with the test solution. Another configuration is Ag/AgCl electrode covered by a porous polymer which is named solid-state reference electrode [Nagy 1997] (Figure 2.6 (b)). The polymer contains aqueous solution which serves as internal solution. Due to the porosity of covering polymer, ions can be transferred between electrode and external solution. This type of electrode has normally more stable potential and longer lifetime compared to the quasi-solid-state electrode. It also does not need filling solution and therefore its miniaturization is simple. However, this configuration of reference electrode is not suitable for long term experiment due to the fast degradation of confined internal solution. Ag/AgCl electrode which is surrounded by a chamber and in contact with internal solution is another type of reference electrode that is termed liquid junction reference electrode (Figure 2.6 (c)). In this configuration, internal solution interfaces with external solution at a porous material which can be a membrane or frit material. The interface restricts the outward diffusion of the internal solution. This way, the concentration of the internal solution remains constant which results in more stable potential. However, the durability of this kind of reference electrodes is limited particularly in miniaturized ones due to the limited amount of reactants. It also suffers from the interface clogging which can generate instantaneous instability in potential [Illingworth 1981]. Ag/AgCl electrode with free-diffusion liquid junction is one of the configurations with capability of producing highly stable and reproducible potential. In this design, the internal solution is flowed through the reference

electrode chamber and comes out through the interface [Dohner 1986, Peters 1997] (Figure 2.6 (d)). The advantages of this system are the constant replenishment of the internal solution, elimination of the liquid junction effect, and fast response. It also prevents the inward diffusion of the external solution and makes electrode insensitive to the dilute external solution.

Initial miniaturization of Ag/AgCl was started by inserting the Ag/AgCl wire in electrolyte using a fine capillary as container. [McGill 1978] used a mixture of concentrated KCl and polyacrylamide gel at capillary tip as a salt bridge with low electrolyte flow rate. In another work, a 1 mm internal diameter glass capillary with tip as small as 1-2 μm was used as container for Ag/AgCl wire with diameter of 0.13 mm [Savinell 1981]. It was used for pH measurement in biological samples. Similarly, [Kitade 2005] used this configuration for potential measurement in confined spaces such as living cells. Ag/AgCl wire was dipped in saturated KCl where polypropylene pipette tip or hypodermic needles were used as reservoir [Pedrotti 1996, Czaban 1976]. They were used as probes for routine pH measurements in microdialysis and clinical pH monitoring. In another version, vapour deposited silver on the outside of capillary glass was converted into silver chloride electrochemically. The outer diameter of capillary was 10 μm [Zhang 1996]. In this configuration, Ag/AgCl wire was replaced with vapour deposited silver which alleviates the typical concerns associated with inserting wire into the electrolyte.

In order to eliminate the effect of liquid junction and need to employing filling soltion in miniaturization process, microfabricated solid-state Ag/AgCl was proposed as a

practical alternative. In this configuration, the filling solution is replaced with a solid-state exchange membrane, for example agar gel, saturated with KCl. It has been performed by spin coat technique [Czaban 1976] and screen printing technique [Simonis 2004] on microfabricated Ag/AgCl thin films. The former reported a notable insensitive electrde to pH in the range of 4-10 and the latter found its potential insensitive to Cl^- concentration in the range of 10^{-6} M to 0.3 M. To prevent reference electrode from effects of dried agar gel, 1-dodecyl-3-methylimidazolium chloride was integrated into a polyvinyl chloride (PVC) matrix [Maminska 2006]. This layer of polymer coated thin layer of Ag/AgCl electrode.The merit along use of this configuration is their capablity to be stored for long period of time after manufacturing process. Similarly in other studies PVC [Yun 2002, Zielinska 2002, Valdes-Ramirez 2005] and epoxy coatings [Nagy 1997] have been utilized to blanket bare Ag/AgCl electrodes and protect them from rapid dissolution in the analyte solution. In order to enhance electrode stability, polyurethane, nafion [Nolan 1997], [Moussy 1999], and silicone rubber coatings [Kwon 2007], have been used as membrane material. However, these gels commonly suffer from poor reproducibility when integrated in solid-state reference electrodes.

Fabrication process of solid state reference electrodes is simpler compared to the other types of microreference electrodes. However, due to limited presence of KCl which is more sever in microscale reference electrodes lifetime of microfabricated reference electrodes is short. Microreference electrodes with microfabricated reservoirs have been proposed in the past few decades. Microfabricated liquid junction reference electrode was integrated with ISFET by etching a cavity in ISFET silicon substrate with a remaining

thin porous silicon membrane [Smith 1984, Smith 1986]. The porous membrane served as a barrier between internal and external solutions and separated electrode from external solution. Thin planar porous glass [Yee 1988], a hydrogel layer [Vanderberg 1990] or a membrane with a pinhole junction [Sinsabaugh 1986] were used in other works to separate internal and external solutions. Effect of filling solution has been found to be notabaly critical where it is concentrated. It has been proved that concentrated filling solution makes dissolution of AgCl layer fast [Yalcinkaya 1997]. There is also a concern about effect of evaporation of filling solution on accuracy of electrode potential over the time of operation. Evaporation of water can be restricted in a liquid ion-exchanger due to the absorption force between water molecules and the mixed poylmer. Liquid ion-exchanger reference electrode have been introduced as suitable replacment of KCl solution by [Maminska 2006], [Thomas 1981], and [Saheb 2006]. This approach may be effective at maintaining constant potential by keeping ion presence at vicinity of the electrode constant.

In terms of microfabrication methods, evaporation and lithography techniques were utilized by [Suzuki 1998] to deposit and pattern Ag in the shape of the electrode. Polyimide layer was used as insulator on Ag electrode in such a way that periphery of Ag is exposed. AgCl layer was then electrochemically grown on edge of Ag and exposed to the internal solution. It was proved that electrode can last for 24 hours with drift of $< 1mV$ (Table 1). Later on, some modifications were applied for example AgCl was grown by dipping Ag in $FeCl_3$ and cellulose acetate layer was incorporated as membrane [Suzuki 1998] and lately electrolyte was replaced with KCl paste [Suzuki 1999].

[Ref.]	Area	Fabrication	Filling solution	Test solution	Stability
[Suzuki 1998]	13mm × 1.5mm	Photolithography sputtering electrochemical oxidation	None (quasi-RE)	0.1 M KCl in 20mM $NaOH/KH_2PO_4$ buffer, pH 7	< 1mV in 24h, 1mV in 8h with saturated AgCl and KCl in solution
[Suzuki 1998]	13mm × 1.5mm	Photolithography electrochemical oxidation, Bulk micromachining	Saturated KCl, AgCl. Pin hole liquid junction	0.1 M KCl in 20mM $NaOH/KH_2PO_4$ buffer, pH 7	<1mV in 3h.
[Suzuki 1999]	13mm × 1.5mm	Photolithography Electrochemical oxidation, Screen printing	Saturated KCl/AgCl. Hydrophillic Polymer liquid junction	0.1 M KCl in 50mM $NaOH/KH_2PO_4$ buffer, ph 7	<2mV in 100h.
[Kim 2006]	N/A	Photo-polymerization for junction polymer	1M KCl. pDADMAC plug junction	PBS at ph 7.4 with 0.15M NaCl	<12mV in 30h.
[Polk 2006]	N/A	Photolithography, lift-off, sputtering, electrochemical oxidation	Saturated KCl in Agarose supporting gel.	10mM KCl, pH range 4-10	<1.5mV in 42h.
[Sun 2006]	2cm× 0.1mm	Electroless plating on glass, electroplating	None (quasi-RE)	3M KCl	<30mV in 14 days
[Huang 2002]	$10^6 \mu m^2$	Photolithography, chemical oxidation	None (quasi-RE)	1mM KCl	<2mV in 5000s
[Suzuki 2000]	1μm dia. capillary	Pre-made capillary & Ag wire. Capillary action for salt bridge and filling solution	3.3M KCl + AgCl	Distilled water	<2 mV in 2400s

[Park 2003]	1.2mm^2	Photolithography, lift-off, Plasma chlorination	None (quasi-RE)	(0.1M Na_2HPO_4, 0.15M NaCl, 0.1 g/l NaN_3 at pH 7.4)	<13mV in 5h
[Simonis 2001]	10mm× 20mm	Screen-printing thick film	None (quasi-RE)	Technical buffer with 0.05mM Cl^-	<70mV in 12h
[Kim 2004]	2mm× 1.8mm	Sputtering, Ni layer added, photolithography, chemical chloridizing	None (quasi-RE)	50mM Tris buffer (pH 7.4) with 3.5M KCl	<1mV in 2h
[Tymecki 2004]	4mm × 24mm	Screen printing	N/A	1 M KNO_3	Drift of < 25 mV in 100h.

Table 2.1 Summary of the performance of microfabricated Ag/AgCl reference electrodes in the literature [Shinwari 2010].

$FeCl_3$ has been proved to be a suitable oxidizer to deposit silver chloride on silver repeatedly in [Yalcinkaya 1997], [Polk 2006], and [Sun 2006].

Using screen printing technology, fabrication of Ag/AgCl paste on low-cost, plastic, and flexible foils has been demonstrated [Tymecki 2004]. Drift of <25mV over 100 hours was achieved with lifetime of 1 week (Table 1). The developed reference electrodes were shown to be compatible with strip potentiometric sensors fabricated in the same format. In other instances, silicon was used as the substrate where Ti and later Pt deposited as seed layer. Following that, Ag/AgCl is screen printed on coated substrate followed by post process treatments [Tymecki 2004, Simonis 2004]. It was suggested by [Simonis 2004] that thicker grain size of silver chloride likely results in more stable performance of Ag/AgCl electrodes.

(IV) Other Microfabricated Reference Electrode:

There are several other electrochemical systems which can be used as reference electrode. Iridium/iridium oxide is a typical pseudo-reference electrode which consists of iridium metal and treated by an oxidizing agent to form an oxide layer. Although microfabrication process of this kind of reference elctrode is well-known, its sensitivity to hydrogen ions remains a major drawback for its application in the test solutions with varied pH [Shinwari 2010]. However, it shows stable potential of 0.52 V in phosphate buffered saline (PBS) solution at pH 7 [Yang 2004, Wang 2002]. In medical and implantable applications, due to its biocompatibilty and high exchange current density, it can be used as reference electrode where pH is predefined and constant [Franklin 2005].

Other reference elecotrdes such as mercury-mercury oxide and mercury-mercurous sulfate electrodes are applicable in area where presence of chlorine ions are not desirable. Copper-copper sulfate electrode is the reference electrode which is used typically to benchmark other electrodes for industrial cathodic protection. Palladium metal is known to have capacity of storing of hydrogen 900 times of its volume in its lattice. Absorption process of hydrogen in palladium consists of formation of three α, $\alpha+\beta$, and β phases. $\alpha+\beta$ phase is known to behave as a hydrogen electrode and therefore responds to pH based on Nernstian relation [Vasile 1965]. In this case, stored hydrogen can evolute from electrode surface and maintain its electrochemical potential stable. Although palladium electrode yields stable performance in $\alpha+\beta$ phase, its initial opertaion in α phase makes its stabilization response long [Wolfe 2005].

2.3.4 DRAWBACKS WITH CURRENT MICROFABRICATED REFERENCE ELECTRODES

Although many attempts have been made to microfabricate reference electrodes, however, current designs still have not overcome some of the main issues as follows. In the case of hydrogen electrode, new techniques such as E-beam deposition have been used to deposit platinum electrodes. However, need to microfabricate gas chamber for hydrogen gas and pressure regulator remains an issue which has not been addressed completely. As mentioned earlier, some groups have tried to replace gas chamber with a conductive polymer which contains hydrogen ions. Nevertheless, complexity of the design and irreproducibility of the potential stays as a disadvantage of this technique [Nann 2000, Kunimatsu 2005].

Calomel reference electrode has been miniaturized by several methods; however, use of gel matrix to incorporate and keep the mercury electrode in place is essential. Since integration of this gel requires special care and is not compatible with microfabrication techniques, so that microfabricated calomel reference electrode is not desirable reference electrode. Moreover, the toxicity of liquid mercury makes calomel electrode an unsuitable candidate for miniaturization [Shibata 1977, Yosypchuk 2003].

Contrary to the standard hydrogen electrode and calomel electrode, silver/silver chloride reference electrode has been investigated widely for miniaturization. Screen printing, electrodeposition, and E-beam deposition of silver has facilitated progress of miniaturization of Ag/AgCl increasingly [Tymecki 2004, Simonis 2004, Polk 2006]. Also, AgCl paste printing, chemical deposition of AgCl, and electrochemically

conversion of Ag into AgCl have been used to microfabricate Ag/AgCl [Tymecki 2004, Sun 2006, Zhang 1996]. However, they were not able to extend lifetime of reference electrode as expected. Usually, drift and fluctuation are associated with the aforementioned microfabricated Ag/AgCl reference electrode due to the limited presence of silver/silver chloride. Some groups tried to protect Ag/AgCl and prevent it from drifting by covering it with porous polymer and using filling solution but complexity of such designs remains an obstacle for their miniaturization [Suzuki 1999]. Finally and most important of all, current microfabricated reference electrodes are not suitable for easy integration. Their complicated integration with devices such as BioFET, make them inappropriate candidates for use in biosensor.

2.4 SUMMARY

In chapter 2 biosensors, BioFET, reference electrode and general applications of reference electrode and its particular application in the BioFET were explained. Microfabricated reference electrode with stable potential which lasts for long period of time is an essential component of the BioFET. Following that, Nernst equation and effective parameters on electrochemical potential was elaborated. The literature survey was done about types, configurations, and techniques which have been used to microfabricate reference electrode by now. It was demonstrated that microfabricated reference electrodes which already present in literature suffer from issues such as instability, irreproducibility, short lifetime, complexity of the process, and incapability of being incorporated with other devices such as biosensors.

Chapter 3

MICROFLUIDIC REFERENCE ELECTRODE

3.1 DESIGN

A microfluidic reference electrode, capable of replenishing its internal solution, is introduced here. The device consists of an electrodeposited coating silver chloride on silver wire. It is embedded into the PDMS microchannel and interfaces with the external solution through the nanoporous polycarbonate membrane (See Figure 3.1). The nanoporous membrane acts as a barrier for diffusion of the internal analytes into the external solution.

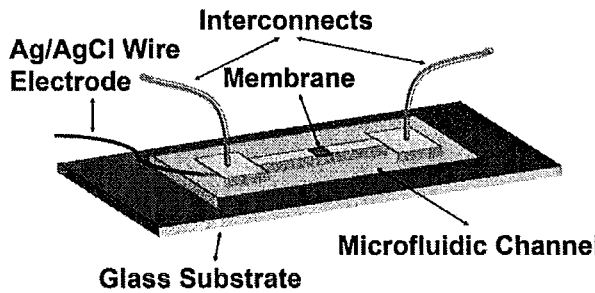

Figure 3.1 Schematic picture of the proposed microfluidic reference electrode.

3.2 ADVANTAGES

Silver/silver chloride type of reference electrode was selected since it has high exchange current density and non-polarisable stable potential in the range of potential which is used in BioFET (as described in chapter 2). Moreover, it is non-toxic and can be microfabricated easier as compared to the other types of reference electrodes. The

microfabrication procedures, which have been used so far, are complex [Suzuki 1999], are irreproducible (10 mV variation in open-circuit potential [Polk 2006]), and has rapid drift (3-4 mV drift per day [Simonis 2005]).The first modification was made by using a bare silver microwire instead of electroplated or screen printed silver. Silver microwire provides sufficient silver during deposition of silver chloride and does not require metallization and printing facilities resulting in a substantial reduction in fabrication cost. The second major modification was made to electrodeposition conditions using high voltage DC and asymmetric potential. This way, the silver chloride structure becomes more porous [Beck 1984] in contrast to the previous silver chloride morphology which was smooth. Finally, in addition to liquid junction configuration, free diffusion liquid junction configuration was designed and used for the first time to overcome the problems associated with liquid junction microreference electrode.

Output potential of the reference electrodes consists of three elements including the bare electrode potential, the potential drop due to the internal solution and the external solution resistance, and finally the potential drop due to the passage of the chlorine in the liquid junction. The net output potential, therefore, is sum of three potentials: (assuming test conditions such as temperature remain constant and there is no external noise imposed by the electric field.)

$$U = U_1 + U_2 + U_3 \tag{3.1}$$

where U_1 represents the bare electrode potential, U_2 represents the potential drop due to the resistance of the solutions, and U_3 is the liquid junction potential. Having known the internal solution concentration, U_1 can be obtained using Nernst equation (assuming

continuous conversion of silver chloride into silver). U_2 may be neglected if conductivity of the solutions are high. U_3 can be calculated as a static variation in reference electrode potential if free-diffusion liquid junction is established by flowing the internal solution through the interface. The above effects are elaborated more in the next section.

3.3 WORKING PRINCIPLE

Observation of the reference electrode performance in its electrochemical equilibrium state without interrupting the reaction at electrode/solution interface is feasible in open-circuit test. It can be performed by drawing slight electrical current through the system and measuring the potential drop.

Overall performance of microfabricated reference electrode is affected by factors including morphology of silver chloride, concentration of Cl^- in internal electrolyte, and finally effect of liquid junction. Stability of reference electrode strongly depends on equilibrium state of electrode/electrolyte interface in which silver chloride (AgCl) coating layer is converted into silver and chlorine based on reaction (2.28). As [Janz 1963] explained, AgCl coating layer can have various structures that could potentially affect the stability of the reference electrode (see Figure 3.2). Their effect on stability of the electrode potential can be attributed to the variation in the local current density. Based on equation (2.18), higher reacting surface of silver chloride reduces the local current density (i.e. j) and subsequently $(E - E^\circ)$ decreases based on equation (2.19). Therefore, the effect of external noise on stability of the electrode potential will be minimized and electrode works at more standardized conditions.

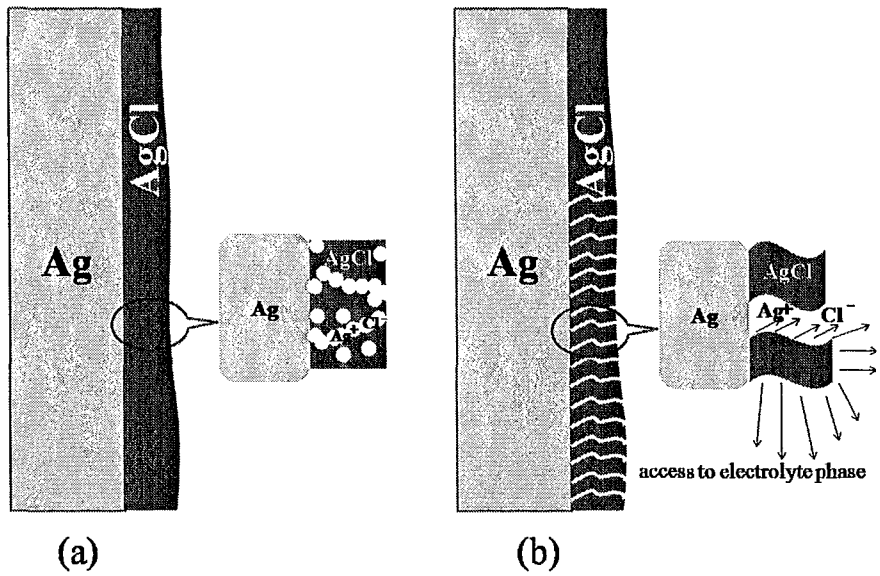

Figure 3.2 Ag/AgCl interface with electrolyte (a) porous (b) high-surface-area AgCl morphology.

Following conversion of silver chloride into silver and chlorine ions, some of the chlorine ions diffuse away from the electrode and simultaneously transfer negative charges. Total transport of ions in the solution can be obtained by Fick's law of diffusion:

$$\frac{dC}{dt} = V\frac{\partial C}{\partial x} + D\frac{\partial^2 C}{\partial x^2} \tag{3.2}$$

where C represents the ionic concentration, t denotes the time, x denotes the distance from a reference origin, V and D are the velocity of the flow of the chlorine and diffusion coefficient, respectively. If the internal solution is kept stationary, the concentration of chlorine ions adjacent to electrode will increase and change the electrode potential. On the other hand, if there is a flow of KCl in the microchannel the internal solution is replaced with new chlorine ions. This way, chlorine concentration remains constant at vicinity of the electrode and therefore reaction (2.28) proceeds in its equilibrium state

resulting in stable potential. The liquid junction potential is what affects the stability of the reference electrode potential also. The potential drop associated with passage of charge through the pores of the membrane depends on several parameters as shown below [Brezinski 1983]:

$$\frac{dU}{dx} = -\frac{RT}{F}\frac{1}{2C}\left(\frac{d\sigma}{dx} + \frac{V}{D}\sigma\right) \tag{3.3}$$

where U represents the potential, R is the gas constant, T is the absolute temperature, F is the Faraday constant, σ represents the concentration of the fixed ion charges on the inner walls of the pores. This equation demonstrates how electric field (dU/dx), fixed ion gradient ($d\sigma/dx$), and bulk flow (V/D) contributions are related. If the fixed ions are distributed uniformly throughout the pores and there is no flow in the junction, U is constant along the pore. Hence, there would be no variation in the liquid junction potential. However, in reality, abrupt change in surface charge of junction always exists. The following relation has been obtained for potential drop in the pore [Brezinski 1983]:

$$\Delta U = \frac{RT}{F}\ln\left[\sqrt{1 + (\sigma/2C_{external})^2} + (\sigma/2C_{external})\right] \tag{3.4}$$

If $C_{external} \gg \sigma$ then $\Delta U \approx 0$, so that there is no effect from the junction. However, for dilute external solution it is not negligible. In this case, $C_{external}$ is comparable with σ and there is a static effect which is induced upon arrival of the flow into the junction. Moreover, there is a dynamic potential variation within the liquid junction when the internal solution concentration changes over the time or the chlorine concentration and/or pH of the external solution vary over the time. The former variation is static and can be merely added to the reference electrode potential (U_3 in equation (3.1)).

The latter variation is dynamic and cannot be predicted during the reference electrode operation.

Flow of internal solution across the membrane has been proposed as an alternative approach instead of a static liquid junction configuration to avoid dynamic variation of liquid junction potential (Figure 3.3). In this case, by assuming negligible effect of uniformly charged junction on concentration gradient within the junction, the following relation is derived from equation (3.2):

$$C = C_{junction} + (C_{external} - C_{junction})e^{-VX/D} \quad (3.5)$$

By substituting equation (3.5) into equation (3.3) and after integration and simplification, the following relation is derived for potential drop across the junction [Brezinski 1983]:

$$\Delta U = \left(\frac{\sigma}{2C_{junction}}\right)\left(\frac{RT}{F}\right)\ln\left(C_{junction}/C_{external}\right) \quad (3.6)$$

Hence, potential drop should be a logarithmic function of concentration of external solution, with a Nernstian slope that is reduced by factor of $\sigma/2C_{junction}$ (Figure 3.4). As $\sigma/2C_{junction}$ is normally several orders of magnitude below unity, effect of external solution on the junction potential should be negligible. Even if external solution is highly diluted, it gives a static variation rather than dynamic variation. Accordingly, it can be deduced that stable and constant potential can be resulted although liquid junction will impose static variation.

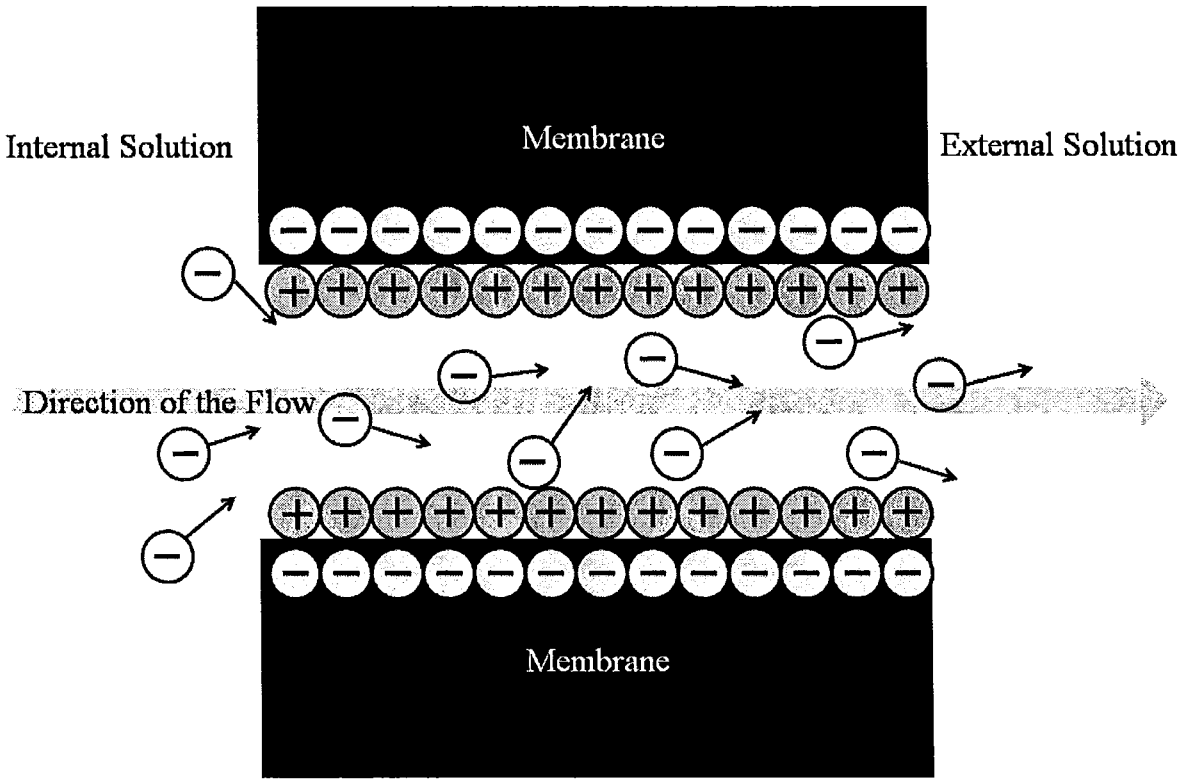

Figure 3.3 Forced fluid flow within membrane pores in presence of stagnated ions on membrane walls.

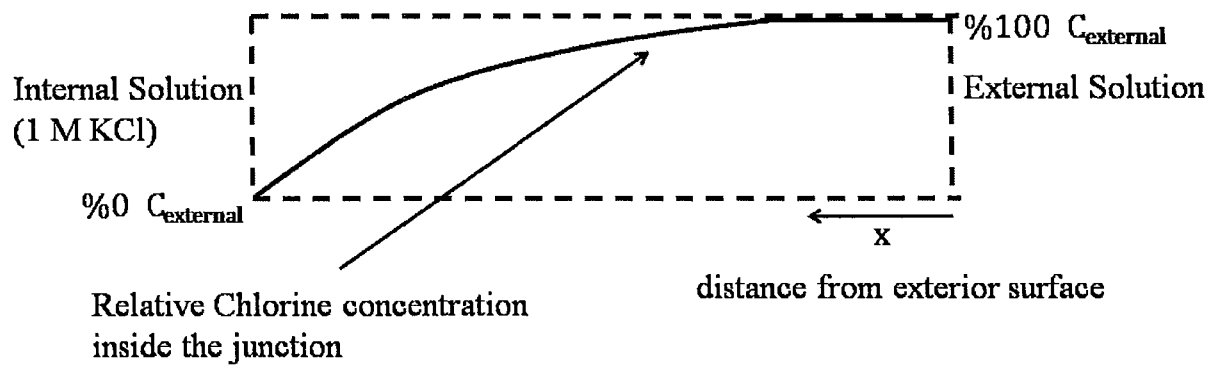

Figure 3.4 External concentration profile during outward flow of internal solution [Brezinski 1983].

3.4 SUMMARY

In chapter 3, the design of the proposed microfluidic reference electrode was described. Three major modifications were made to previous microfabricated reference electrodes including use of microwire instead of printed and electrodeposited silver, modified electrodeposition of the silver chloride, and operation of the microfluidic reference electrode in different modes. The aforementioned modifications were applied to improve the stability of the overall potential of the reference electrode.

The overall performance of reference electrode is function of some factors such as, Ag/AgCl morphology, filling solution, and liquid junction. Ag/AgCl morphology with higher surface area can reduce variation of the local current density which can potentially introduce noise to the electrode/electrolyte interface. The filling solution (internal solution) effect is significant when concentration of the chlorine varies during the operation period. High concentrated or replenished internal solution can retain the stability of the reference electrode potential. Finally, liquid junction can impose static and dynamic instabilities on the reference electrode potential particularly in dilute external solutions. Flow of the internal solution within the liquid junction was shown to be a suitable configuration to offset the liquid junction effect.

Chapter 4

DEVICE FABRICATION

4.1 INTRODUCTION

Microfabrication of the reference electrode is a multi-step process which includes anodic deposition of silver chloride on the silver wire, fabrication of the PDMS microchannel using soft-lithography technique and finally assembly of the device by microcontact printing. In this chapter, the materials and fabrication techniques are described first. A novel fabrication of bare Ag/AgCl electrode is introduced and, following that, microfabrication process flow including master mold fabrication and device assembly is described.

4.2 MATERIALS

4.2.1 SILVER WIRE

High purity silver wire (>99.99%) with diameter of 200 μm was purchased from Harvard Apparatus Canada (6010 Rue Venden, Abeele Saint, QC H4010). Silver microwire was chosen because of its ease of integration, amount of silver present and multi-grained annealed surface that produces uniform AgCl films.

4.2.2 Si WAFER

3″ mechanical grade Si wafer with thickness of 500 μm was purchased from University Wafer (66 N Street, Unit #9, South Boston, MA 02127 USA). The Si wafer is

a pure silicon substrate which comes in different size, crystal orientation, and grade. In the current study, it was used for the master mold fabrication and microcontact printing purposes which do not impose any specific requirements on Si wafer selection.

4.2.3 SU-8 PHOTORESIST

Su-8 is an epoxy based negative photoresist which can be cured by UV light. It is widely used for producing high aspect ratio and high mechanical strength microstructures. Su-8 of various viscosities is available from MicroChem Corporation (90 Oak St., Newton, MA 02464, USA). Su-8-100 is capable of forming microfeatures with thickness of 50-250 microns which is suitable for current study. In this thesis, Su-8-100 was patterned in shape of microchannel on Si wafer to fabricate master mold. Before exposure to UV light, Su-8 photoresist is in a viscous liquid state. Su-8 viscosity (hence the film thickness that can be produced) varies depending on the percentage of the solid content presents in it [Feng 2003]. Su-8 polymerization occurs in two steps. The first step is during UV exposure and the second step is during post-baking process at pre-determined temperature.

4.2.4 POLYDIMETHYLSILOXANE (PDMS)

Polydimethylsiloxane, known as PDMS, is a transparent polymer which has been used widely in the past decade for microfluidic device fabrication due to its unique advantages such as transparency, biocompatibility, user-defined stiffness, and ability to replicate in nanometer size features [McDonald 2002, Satyanarayana 2005]. Its excellent

properties in microcontact printing and sealing off the gaps led us to use it in the device structure fabrication and sealing procedure.

PDMS pre-polymer was purchased from Dow Corning Incorporation, USA (distributer in Canada: 5109 Harvester Road, Unit B3, Burlington, ON L7L5Y9), supplied as two separate components (base and curing agent). Polymerization of base takes place in presence of curing agent and is speeded up by heating up the mixture. Base (long chains containing vinyl groups) is cross linked with a curing agent containing hydrosiloxane group [Fu 2003]. After curing process, the product is a transparent solid silicone elastomer. Ratio between base and curing agent determines the solidified PDMS elastomer stiffness. Higher percentage of the base results in more viscous PDMS pre-polymer and softer solidified PDMS. Adding more curing agent cross links more chains of base resulting in stiffer solidified PDMS. Ratio of 10:1 base to curing agent has been recommended by supplier as a suitable blend of base and curing agent for fabrication of the device structure. For microcontact printing purposes, a thinner layer of PDMS adhesive layer was obtained by adding higher percentage of curing agent (1:3 base to curing agent, see section 4.6).

4.2.5 POLYCARBONATE MEMBRANE

Nanoporous polycarbonate membranes (6μm thickness) with various pore sizes were purchased from GE Osmonics company (GE Osmonics Labstore, 5951 Clearwater Dr Minnetonka, MN 55343, USA). As provided by the supplier, the pore size distribution falls between +0% to -20% of the nominal size. The pore density is 4×10^8 per cm^2 and

6×10^8 for 100 nm and 50 nm (and 10 nm) pore size, respectively (±15% tolerance of the nominal pore density). Polycarbonate membrane can be integrated with other polymeric parts using PDMS as adhesive material. It was used as an interface between internal and external solutions in order to restrict outflow of internal Cl^- ions.

4.2.6 KCL

Potassium chloride (KCl) was used both for silver chloride formation as well as the internal solution in the reference electrode. KCl powder was purchased from Caledon Laboratories (Georgetown, ON L7G4R9). KCl was selected as the electrolyte during silver chloride deposition. It is an equitranferent solution in which its constituents (e.g. potassium and chlorine) have similar diffusion coefficient [Brezinski 1983]. Thereby, it can be also used as a suitable internal solution without interference of K^+ on liquid junction potential [Brezinski 1983]. Furthermore, its concentration was set to be 1 M in order to prevent solution from crystallization within the junction and clogging the membrane. Electrochemical potential of electrode in 1 M KCl has less thermal dependency as opposed to the saturated KCl while being concentrated enough to keep internal chlorine concentration constant. Additionally, dissolution of AgCl is faster in 3 M KCl which shortens the lifetime of the electrode [Yalcinkaya 1997].

4.3 FABRICATION METHODS

4.3.1 SOFT-LITHOGRAPHY

Soft-lithography technique was used to fabricate the microchannel. It has been utilized and characterized widely in the past two decades [McDonald 2002]. It is also a low-cost process and allows consistent replication of the device.

4.3.2 MICROCONTACT PRINTING

Microcontact printing was used to attach the nanoporous membrane onto the microchannel and define the open interface that bridges the internal and external solutions. The advantage of this method is that the patterning of the membrane is precise which allows reproducible device fabrication [Wu 2005].

4.4 SILVER/SILVER CHLORIDE ELECTRODE FABRICATION

As mentioned in chapter 3, silver chloride structure can have porous or particular nanostructure shape with high surface area. The latter morphology can provide higher reaction surface area which is desirable for stability of the reference electrode potential (section 3.3). To achieve this kind of morphology, higher DC potential was applied to speed up the silver chloride formation and increase the reaction surface area. In addition, AC mode deposition at high voltage was employed to investigate effect of frequency and cathodic potential on silver chloride formation. Increasing either aforementioned factors can generate silver chloride with porous morphologies.

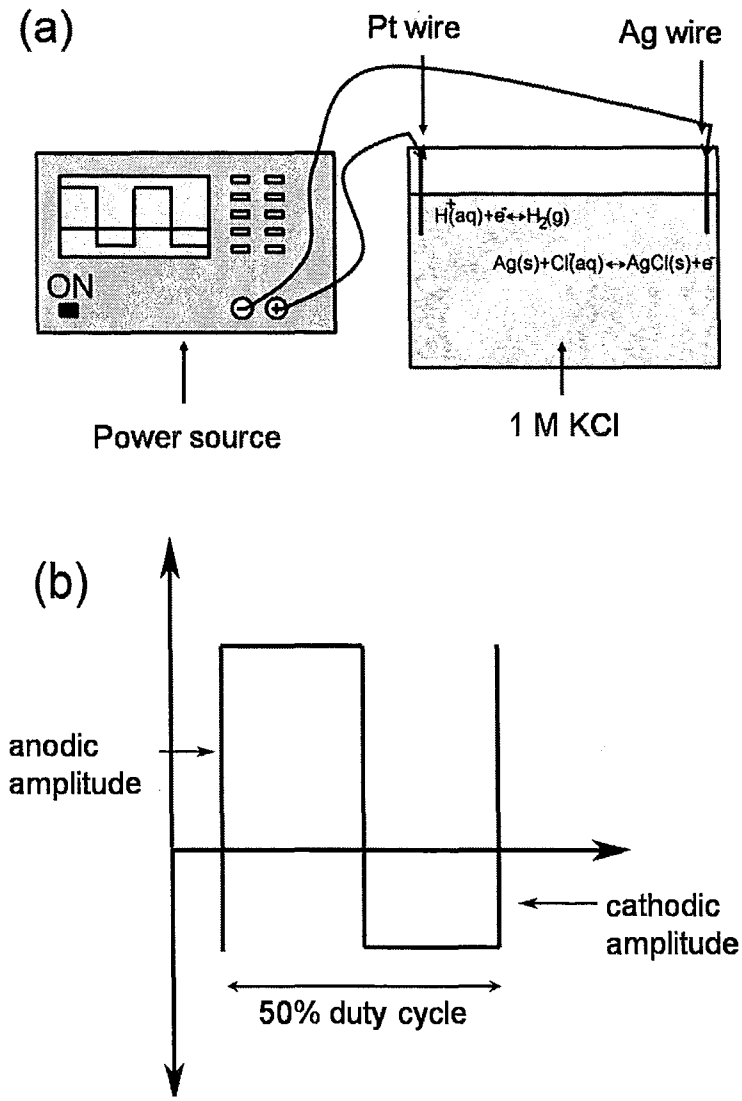

Figure 4.1 (a) Schematic demonstration of fabrication set up consisting of anodic electrodeposition of silver chloride on silver wire against platinum wire in 1 M KCl for 15 min (b) waveform definitions.

In order to understand their effects, electrochemical deposition of AgCl was performed on the portion of Ag wire (1 cm) that was dipped in KCl using constant DC voltage as well as asymmetrical square waveforms. The fabrication setup of Ag/AgCl electrode is as shown in Figure 4.1 (a). It consisted of a function generator (Tektronix AFG 3022B) that

is capable of generating square voltage waveforms of 50% duty cycle with various frequencies and anodic/cathodic amplitudes (Figure 4.1 (b)). A DC power source (Keithley 2636) was used for electrodeposition in DC mode. The power sources were connected to an electrochemical deposition system consisting of platinum wire as cathode (250 μm in diameter) and silver wire as anode (200 μm in diameter), spaced 1 cm apart and immersed in 1M KCl solution. Before the deposition, silver wire was rinsed by acetone and dilute HCl with DI water rinse in between to remove organic and inorganic residues on silver surface (see appendix 1 for more details). In addition, the chemical deposition method was also used to fabricate Ag/AgCl electrode. In this method, a defined length of Ag wire was dipped in 100 mM $FeCl_3$ (as a strong oxidizer) for 1 hour to convert Ag into AgCl. The stability results are presented in chapter 5.

4.5 MASTER MOLD FABRICATION

Photomask was designed in SolidWorks software (Dassault Systèmes SolidWorks Corporation) and printed on transparency sheet. The microchannel pattern consisted of two reservoirs (5mm x 5mm) which were bridged by a rectangular channel (500μm x 3cm, Figure (4.2)). Si wafer cleaning procedure was performed by dipping the wafer in acetone followed by methanol for 20 seconds for each step. The wafer was rinsed by DI water for 5 minutes and placed on hot plate at 110°C for 2 minutes. Following that, the wafer was placed in the oxygen plasma at 50 Watt exposure for 1 minute in order to remove inorganic residue on the top surface. Afterwards, Su-8-100 photoresist was spun on the wafer at 500 rpm for 30 seconds followed by spinning at

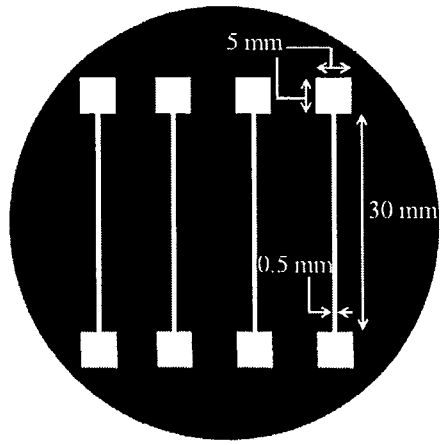

Figure 4.2 Photomask.

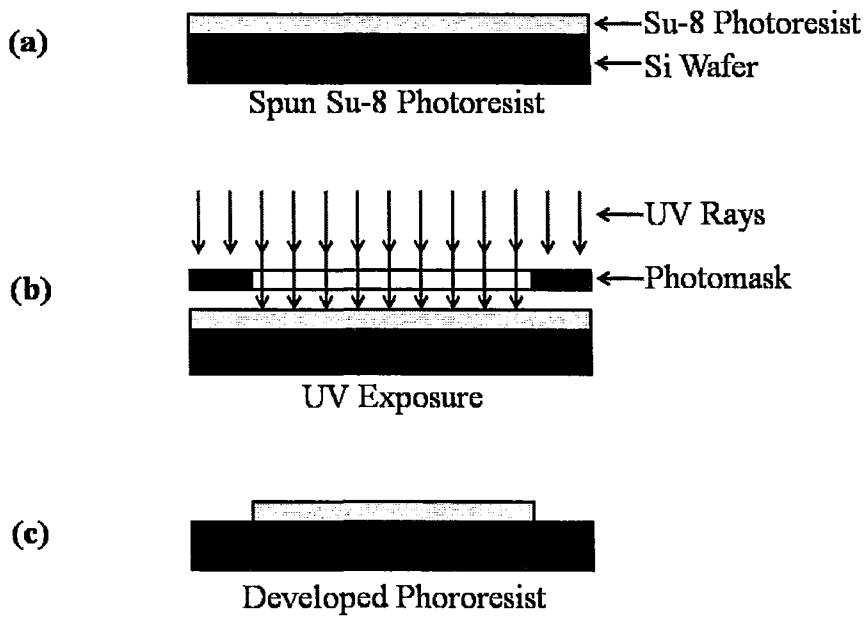

Figure 4.3 Master mold fabrication process flow.

1700 rpm for 40 seconds to obtain 80μm thick layer (Figure 4.3 (a)). It was prebaked for 12 minutes at 65°C and the temperature was increased 10 degrees per minute up to 95°C at which the wafer was baked for 1 hour. After that, the photomask and wafer were

aligned under a mask aligner and exposed to UV (365 nm) with power of 6.8-mWatt for 95 seconds (Figure 4.3 (b)). After exposure, the post-baking was performed at 65°C for 5 minutes and temperature was ramped 10°C per minute up to 95°C at which the photoresist was baked for 10 minutes. After baking, unexposed area of the photoresist was developed for 30 min using the developer (mixture of ethyl lactate and diacetone alcohol) (Figure 4.3 (c)). The wafer was rinsed with Isopropyl alcohol (IPA) to ensure complete removal of uncured Su-8, see Figure 4.4 (see appendix 2 for more details).

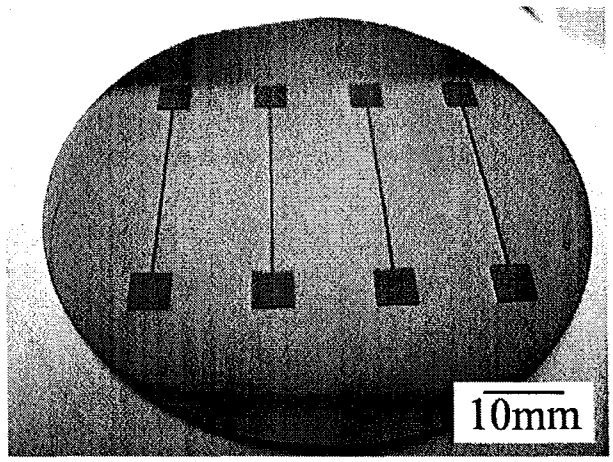

Figure 4.4 Mold.

4.6 MICROCHANNEL FABRICATION AND DEVICE ASSEMBLY

PDMS microchannel was obtained by casting PDMS pre-polymer (base/curing agent: 10/1) at 80°C for 2 hour on the mold fabricated in the previous step (Figure 4.5 (A-B)). The top surface of the microchannels were cleaned in oxygen plasma at 50 Watts for 1 min (4.5 (C)). In order to attach a nanoporous membrane on the microchannel, a thin layer of PDMS was obtained by spinning PDMS pre-polymer

(base/curing agent: 1/3) on the silicon wafer at 10000 rpm for 4 minutes. The microchannel top surface was placed on the thin uniform PDMS pre-polymer and lifted off (Figure 4.5 (D)). This way, the top surface of the microchannel was adhesive enough to bond the membrane on it. Following that, Ag/AgCl wire was inserted into the reservoir of the microchannel by a needle (Figure 4.5 (E)). Then, the polycarbonate membrane was laminated on microchannel top surface (Figure 4.5 (F)). In order to pattern the nanoporous membrane and define the open interface area, another PDMS microchannel was utilized as a microcontact printing stamp. It was placed on the PDMS adhesive layer and aligned perpendicular to the underlying microchannel to print the PDMS pre-polymer on the membrane.

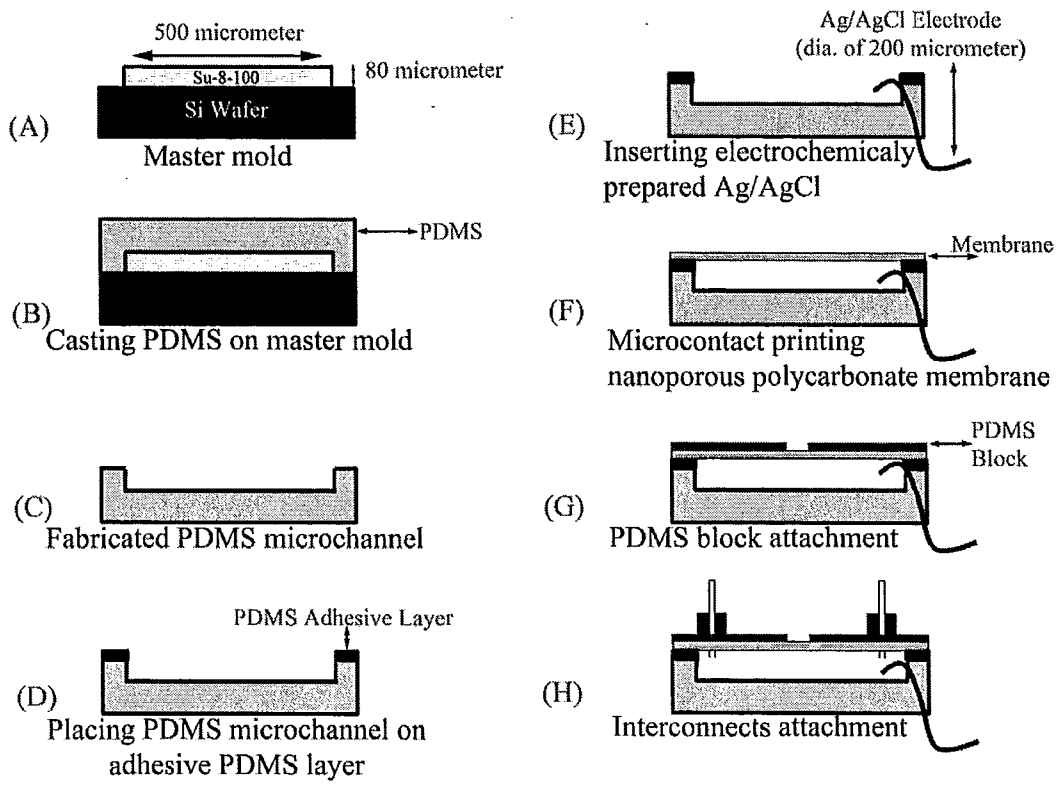

Figure 4.5 Process flow of device fabrication.

Thus, the membrane pores in the printed area are blocked by PDMS pre-polymer and only a 500 μm x 500 μm area of the membrane has its pores open (Figure 4.5 (G)). The open area serves as the interface to the external analyte during the mircrofluidic reference electrode operation (Figure 4.6). Finally, a PDMS top layer (2 cm wide, 5 cm long, 1 mm thick) with a central opening for the open area of the membrane and two holes (1.2 mm in diameter) for interconnects was bonded onto the membrane using the microcontact printing to enclose the microchannel. The device was cured at 80°C for 4 hours. Two PDMS blocks (1 cm wide, 1 cm long, 5 mm thick) with central holes (made by punch, outer diameter of 1.2 mm, Harris company, Capitol Scientific Inc., 2500 Rutland Drive, Austin, TX 78758, USA) was made and interconnects (plastic tubes with inner diameter of 0.8 mm and outer diameter of 1.2 mm) were placed in punched area. Following that, PDMS blocks were attached to the PDMS top layer of the device by the PDMS pre-polymer and cured at 80 C° for 2 hours (Figure 4.5 (H)). In the next step, the Ag/AgCl electrode was shielded by a plastic tube (inner diameter of 1.6 mm, Tygon, Tubing, Fisher Scientific Company, 711 Forbes Avenue, Pittsburgh, Pennsylvania 15219, USA) and PDMS pre-polymer at connection area. Following that, it was cured at 80°C for 2 hours. The final device has planar structure and is suitable for integrated with BioFET reservoir as explained in section 2.2. The open region of the membrane has micro-scale area which fits the BioFET reservoir. The final device is presented in Figure 4.7 (see appendix 3 for more details).

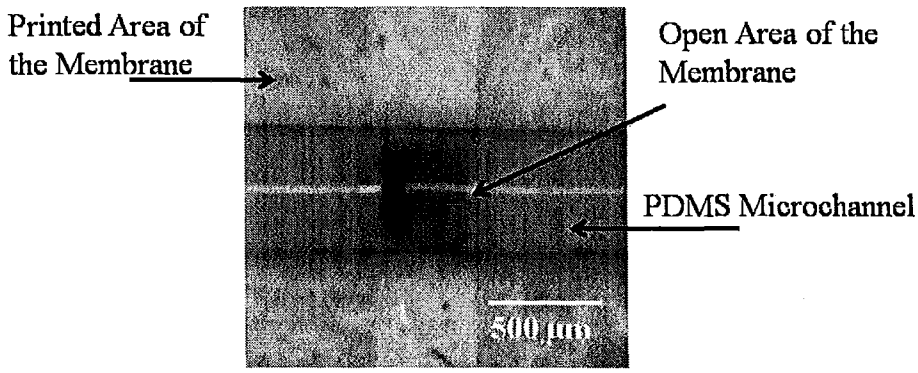

Figure 4.6 Microcontact printed polycarbonate membrane.

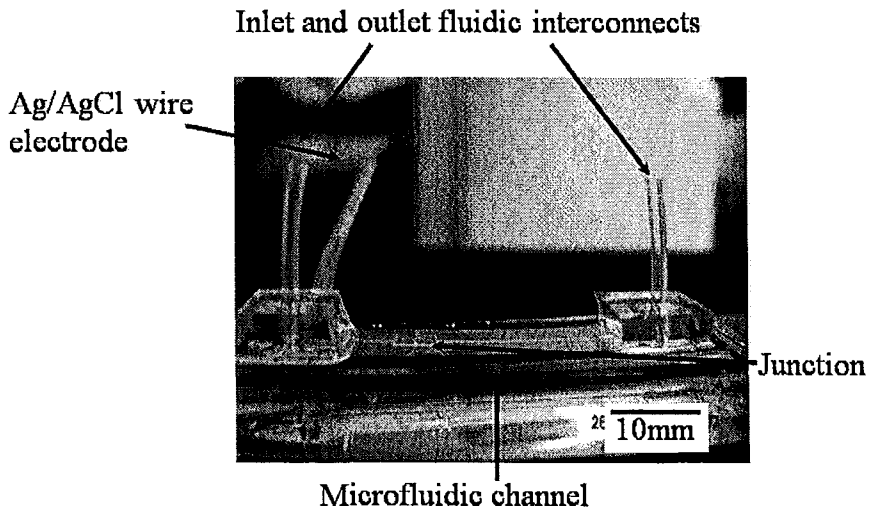

Figure 4.7 Final device.

4.7 SUMMARY

In chapter 3, the material and microfabrication techniques used in this thesis were introduced and described firstly. Then, the fabrication procedure of the bare silver/silver chloride, using both anodic electrodeposition and chemical deposition of silver chloride, was described. In the former technique, both DC and AC modes of deposition were utilized to electrodeposit AgCl in KCl solution and in the latter technique $FeCl_3$ was used as oxidizer. In the next step, the master mold was fabricated using the soft-lithography technique. The PDMS microchannel was made by casting PDMS pre-polymer on the master mold. Using the microcontact printing technique, a nanoporous polycarbonate membrane was bonded onto the microchannel to separate the internal microchannel from the external medium. At the final step, using adhesive PDMS pre-polymer, interconnects were attached onto the microchannel to introduce the internal solution.

Chapter 5

TEST SET UP AND RESULTS

5.1 TEST SET UP

Open-circuit potential (OCP) measurement of the bare Ag/AgCl electrode was performed by immersing the AgCl region of the bare Ag/AgCl wire in phosphate buffer saline 10X (PBS) and measuring its OCP against the commercial Ag/AgCl reference electrode (Sigma Aldrich Canada), that has an internal solution of saturated 3.5 M KCl. Similarly, the microfluidic reference electrode was held in PBS solution using laboratory clamp and tested in 3 configurations as follows: Figure 5.1 (a) shows microfluidic reference electrode configuration, where the internal reference solution (1M KCl) was kept stationary. This configuration is referred to subsequently as the stationary liquid junction configuration. Figure 5.1 (b) shows the configuration where a flow could be initiated, by means of a syringe pump, across the nanoporous membrane. This type of reference electrode is termed, hereinafter, the free-diffusion liquid junction. In a third configuration, the internal solution was made to flow from the inlet to the outlet of the microchannel. This is referred as flow of the internal solution inside the microchannel. Two modes were investigated where the fresh solution arrives at the porous interface before reaching the Ag/AgCl wire (Figure 5.2 (a)) and the other where it reaches the wire before arriving at the porous interface (Figure 5.2 (b)). All the internal solution was filtered by 450 nm pore size filter to eliminate particles and bubbles that could clog the membrane.

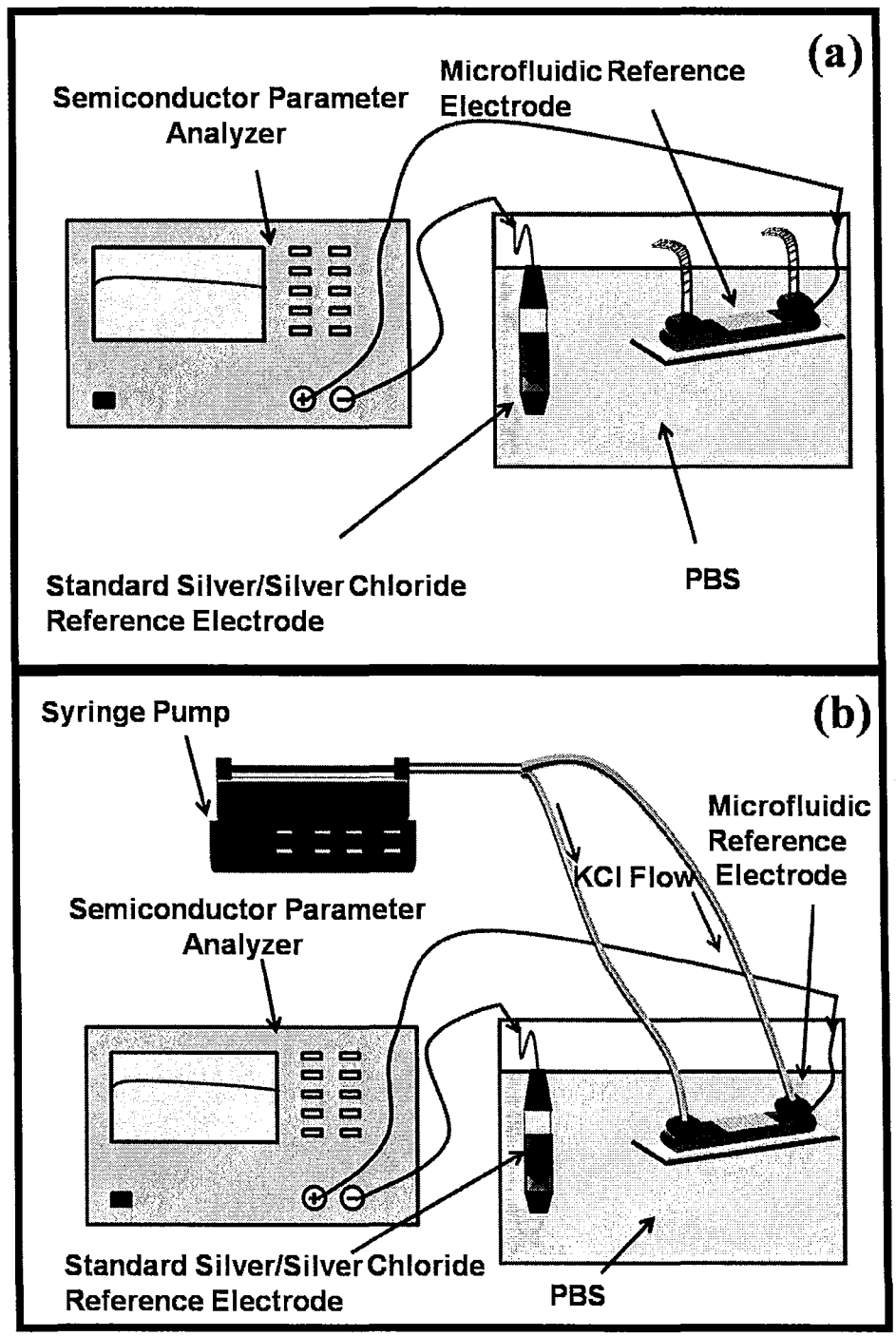

Figure 5.1 Schematic of stability test set up of microfluidic reference electrode with (a) stationary liquid junction (b) free-diffusion liquid junction.

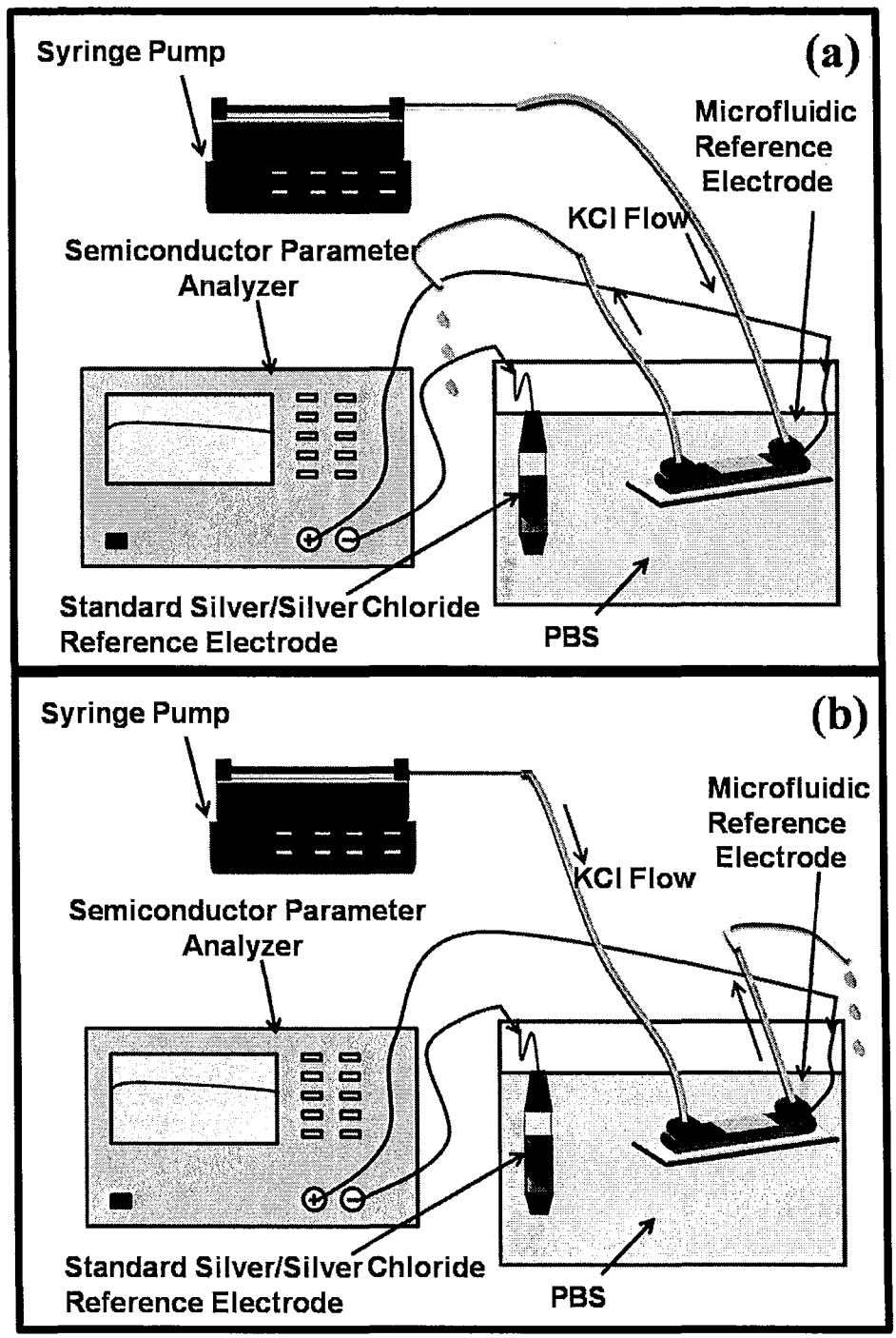

Figure 5.2 Schematic of stability test set up of microfluidic reference electrode with flow of internal solution (a) arrives at the porous interface before reaching the Ag/AgCl wire and (b) it reaches the wire before arriving at the porous interface.

An Agilent 4156C semiconductor parameter analyzer was used to measure the open-circuit potential. It imposes a small current (~400 pA) and measures the potential difference between the microfluidic reference (or bare) electrode and a macroscale commercial reference electrode. The time step of data acquisition was set to be 65 sec (which was the maximum interval between data points). To calculate the electrode potential stability range, the entire operation time was divided into 1 hour slots and, following that, the data in each window was averaged. The electrode potential was considered to be stable if the ratio of the change in the 1 hour average potential over adjacent time interval does not vary by more than 1% (see equation (5.1)).

$$|Avg_{n+1} - Avg_n|/Avg_n \geq 0.01 \quad (5.1)$$

The standard deviation of the potential within the 1 hr averaging window was computed, and this standard deviation was averaged over the lifetime of the electrodes to obtain the stability of its potential. The difference between the maximum and minimum potential in the stable range was used to obtain the potential drift.

Depending on the configuration of the microfluidic reference electrode, some pre-treatments are essential. In the stationary liquid junction reference electrode and configuration of flow of KCl through the microchannel, the inlet and outlet were connected to an evacuated chamber to make a pressure difference between the microchannel and ambient air. At the same time, several KCl droplets was left on the open area of the membrane to fill the pores (Figure 5.3 (a)). Then, the microchannel was disconnected from the evacuated chamber and filled with 1 M KCl and the external surface of the open region membrane was kept in contact with 1M KCl (Figure 5.3 (b)).

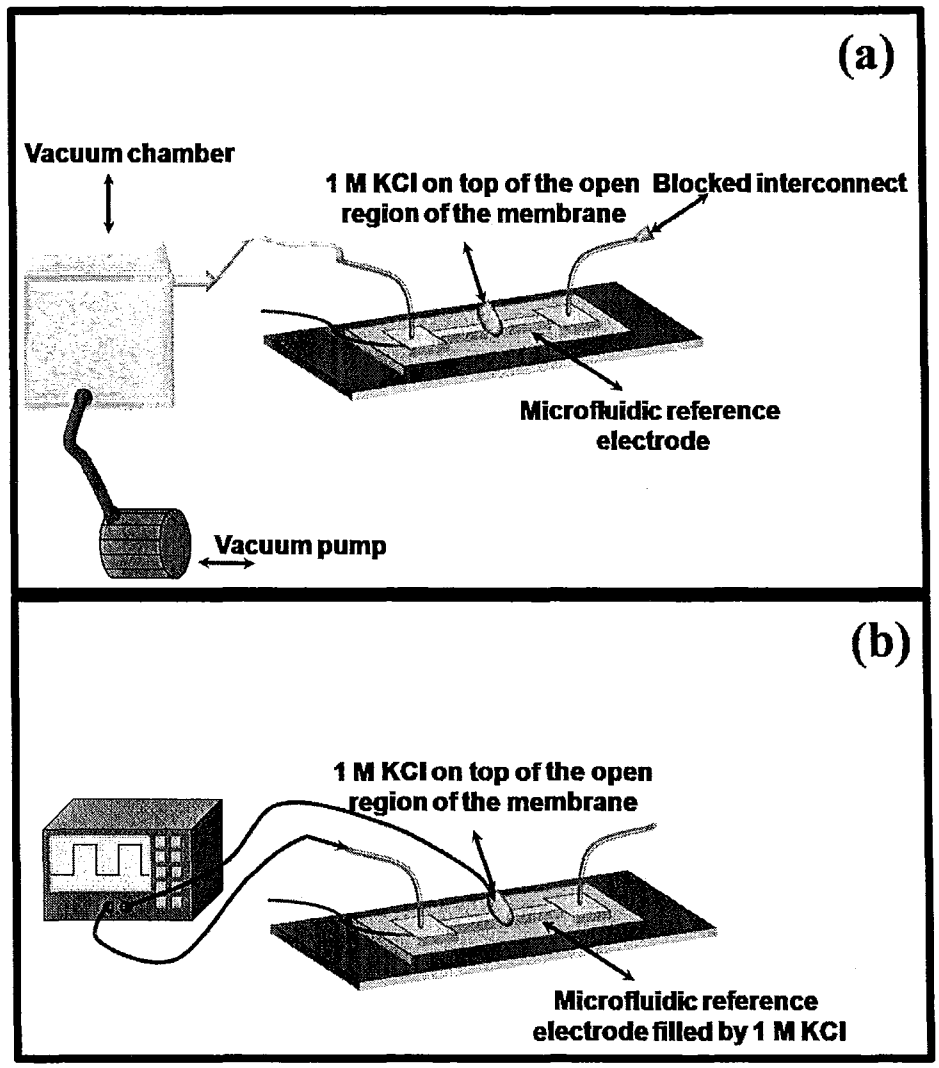

Figure 5.3 Schematic of pre-treatment set up of microfluidic reference electrode (a) Evacuated microchannel (b) Asymmetric potential was applied between two sides of the membrane.

An asymmetric potential (anodic and cathodic potential of 5 V and duty cycle of 50% and frequency of 1 Hz) was applied between the internal solution and the external KCl for 10 minutes (Figure 5.3 (b)). It facilitates removal of trapped air in the pores and filling them with the internal solution (1 M KCl) that can shorten the initial stabilization time. In the free-diffusion liquid junction case, in addition to the explained pre-treatments and in

order to establish a steady-state flow of the internal solution inside the pores, the internal solution with a flowrate of 2 μL/ hr was flowed through the membrane for 5 hours before the actual experiment.

5.2 RESULTS AND DISCUSSION

5.2.1 CHARACTERIZATION OF BARE Ag/AgCl ELECTRODE

The effect of silver chloride morphology and its preparation method on electrode potential stability was studied by growing silver chloride on silver wires at various conditions. Subsequently, its open-circuit potential stability was measured against the macroscale calomel reference electrode (Fisher Scientific, internal solution is saturated 3.5 M KCl) in 1 M KCl. Figure 5.4 shows the open-circuit potential measurement of the bare Ag/AgCl electrode versus the commercial Ag/AgCl reference electrode in PBS 10X solution. In this experiment, two methods (chemical and electrochemical) of AgCl formation on the Ag wire were used to identify the one that provided a more stable potential and longer life time. The electrochemical deposition was performed by 1 V DC anodic potential on silver wire in 1 M KCl against platinum wire with 1 cm spacing for 15 minutes. Chemical deposition was done by dipping the Ag wire in $FeCl_3$ for 1 hour (see section 4.4). For each experiment, 3 samples were tested. It can be seen that the former technique provides longer lifetime (~63hrs) in comparison with the latter (~6hrs) with the same potential stability.

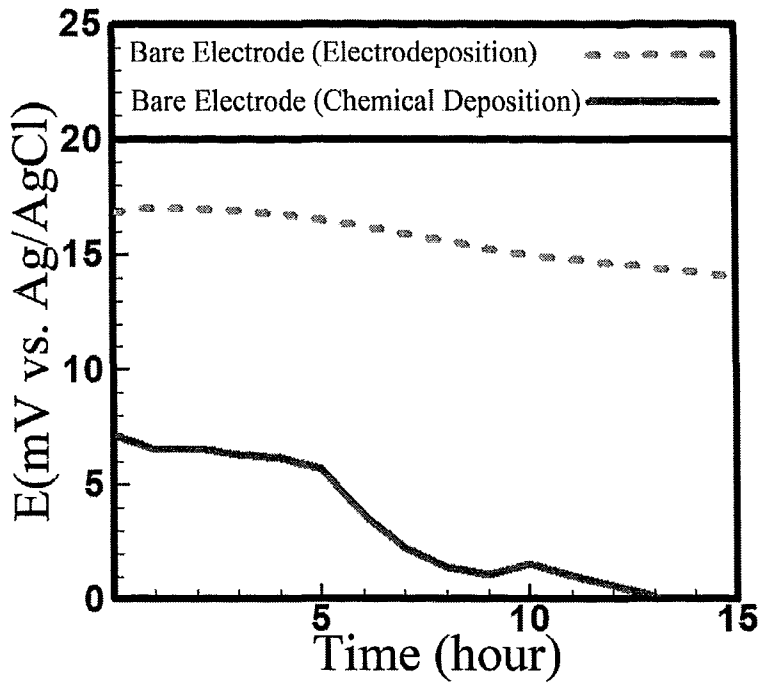

Figure 5.4 Stability test of bare Ag/AgCl electrode in PBS 10X.

(I) Effect of Electrodeposition Conditions on AgCl Morphology

Next, we investigated the use of constant potential and various electrical signal waveforms to electrodeposit AgCl on silver wire and its impact on the morphology of deposited AgCl and stability of its potential. The first set of experiments was conducted using a DC voltage of 0.5V-3V. AgCl was anodically grown on silver wire in 1 M KCl against a platinum wire with 1 cm spacing for 15 minutes. As seen in Figure 5.5 (a), at 0.5 V, AgCl does not cover the entire surface. The morphology, obtained at this voltage, is globular, which comprises of grains of ~500 nm. At 1 V, the entire surface is covered by nanosheet structures with some globular structures interspaced (Figure 5.5 (b)). The size of the globular grains was found to be between 500 nm-1 μm in diameter while the size of the nanosheets was found to be 3-5 μm high, 10-15 μm in long, and ~300-400 nm

thick. At 2 V anodic potential, the silver wire is covered mostly by the nanosheets, which are 300-400 nm thick, 5-10 μm high, and 10-20 μm long (Figure 5.5 (c)). Similarly at 3 V, the wire is fully covered by nanosheet structure that are 300-400 nm thick, 10-15 μm high, and 15-25 μm long. In summary, the results indicates that growth of the nanosheet AgCl structure instead of conventional globular structure, occurs at high anodic DC potential (>0.5). Increasing the anodic potential substantially enlarges the grown nanosheet.

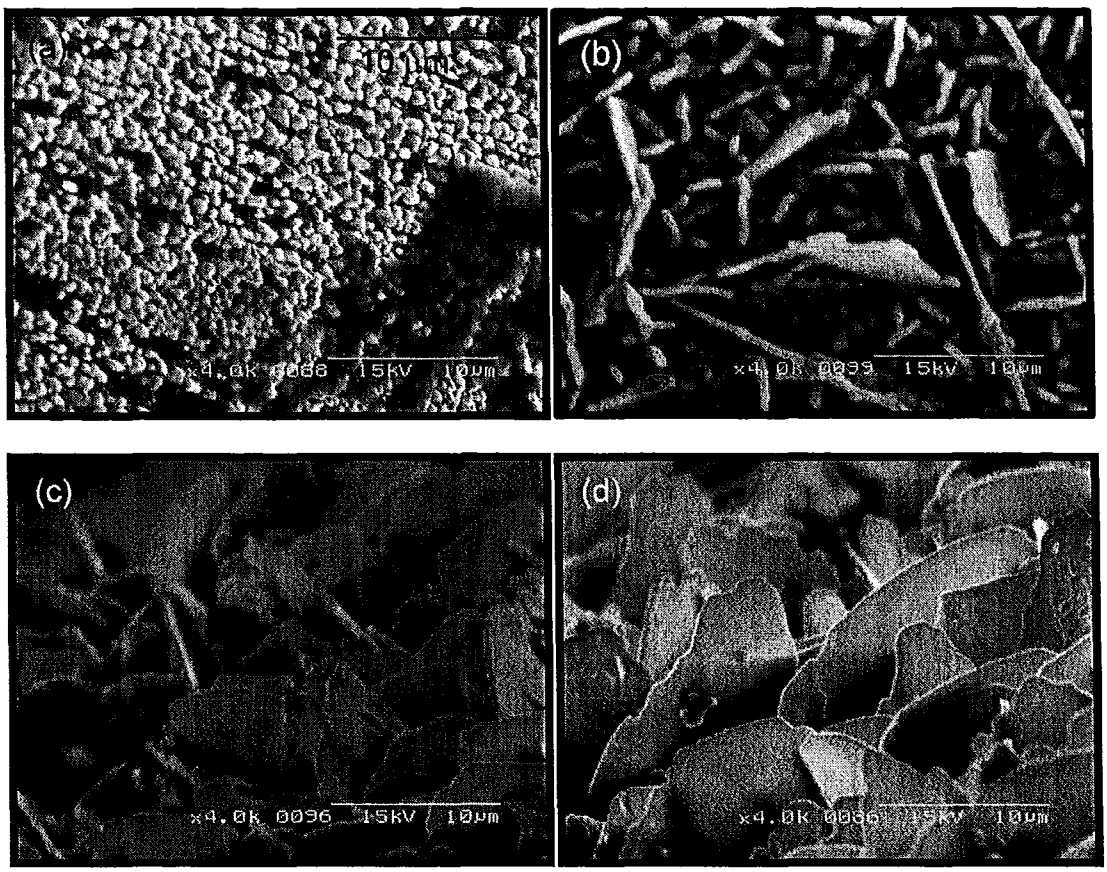

Figure 5.5 SEM pictures of anodically grown silver chloride on silver wire in 1 M KCl against platinum wire with 1 cm spacing by different voltages in DC mode (a) 0.5 V (b) 1 V (c) 2 V (d) 3 V for 15 min. (The scale bar in the top right corner of the composite image applies to all individual images.)

As explained in section 4.4, the frequency and cathodic voltage can affect the silver chloride morphology. Among the various waveforms, an asymmetric waveform was chosen to ensure that a constant potential is applied during anodic charging and cathodic discharging. This eases the study of reactions occurring during anodic and cathodic processes. Therefore, in order to test the effect of frequency on the electrodeposited silver chloride morphology, an asymmetric potential with various frequencies and following specifications was applied: 2 V anodic potential and -200 mV cathodic potential in 1 M KCl against a platinum wire with 1 cm spacing. Similar to the DC mode, the growth of nanosheet silver chloride on silver wire was observed by SEM pictures at low frequency, i.e., 0.5 mHz and 0.5 Hz (Figure 5.6 (a-b)). The size of nanosheets was found to be 200-300 nm in thickness, 3-4 μm in height, and 5-10 μm in length. For the same voltage magnitude but higher frequency, e.g., 50 Hz and 50 kHz globular structure was obtained which varies between 100 nm to 500nm in diameter (Figure 5.6 (c-d)).

Nanosheets of silver chloride are found to be slightly slanted (~80^{o}-90^{o}) with respect to the wire surface. Moreover, they do not intersect each other at a constant angle and space between them is filled by a fine globular layer (300-500 nm in diameter). By a quantitative analysis of the images obtained by SEM, it is deduced that the size and distribution of the nanostructures depends on the most prominent parameter which has a direct influence on the morphology of the surface, i.e., frequency. At a frequency higher than 50 Hz (Figure 5.6 (c-d)), there is a noticeable reduction in the volume fraction of the sheets. It should be noted that until frequency is 50 Hz, the height of the sheets decreases

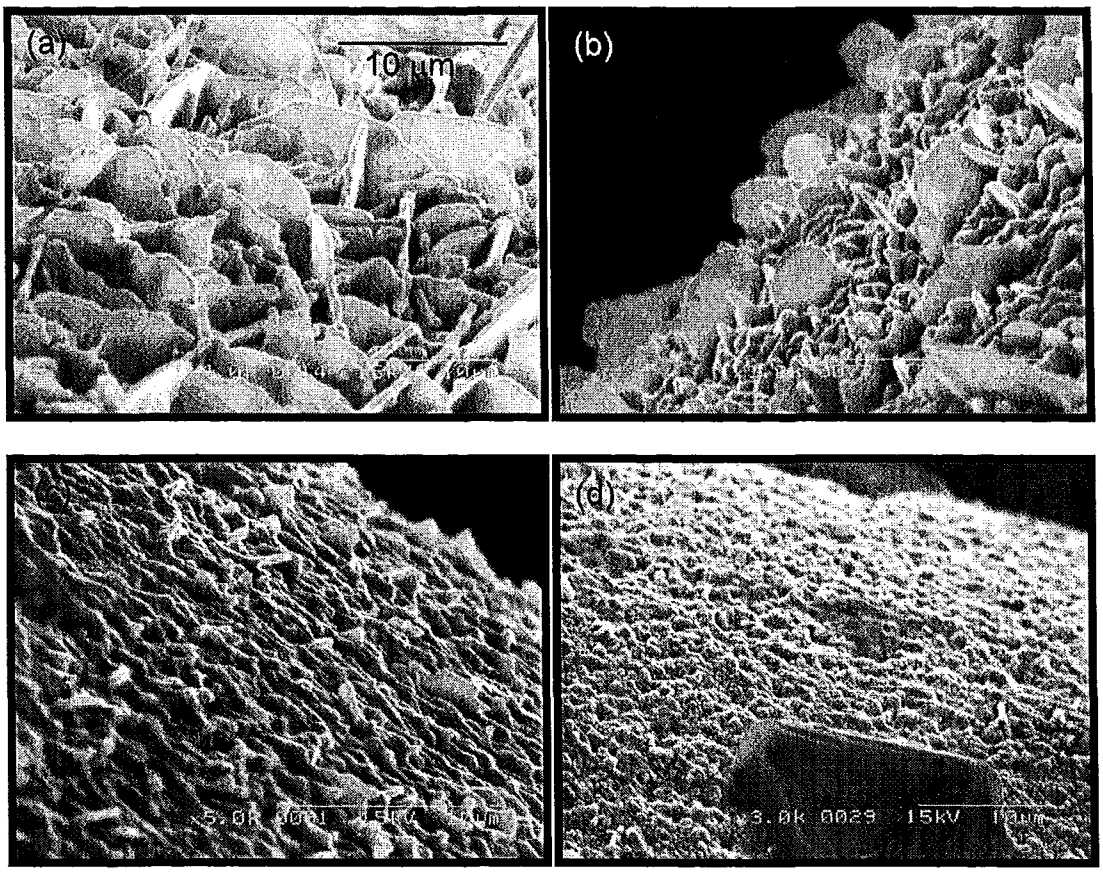

Figure 5.6 Side SEM views of anodically grown silver chloride on silver wire in 1 M KCl against platinum wire with 1 cm spacing by applied voltage of 2 V and -0.2 V as anodic and cathodic potentials, respectively while frequency was (a) 0.5 mHz (b) 5 Hz (c) 50 Hz (d) 50 kHz and employed for 15 min. (The scale bar in the top right corner of the composite image applies to all individual images.)

from ~4 µm to ~1-2 µm. In fact, these sheets start vanishing after 5 Hz followed by the appearance of globular structure. In summary, the microstructure is refined more and more when the frequency increases. For the highest frequency, the globular AgCl structure is clearly formed.

To obtain a tentative understanding of the anodic potential-frequency relationship, the silver chloride was deposited on the silver wire by applying various anodic potential and constant cathodic potential of -200mV in M KCl versus the platinum

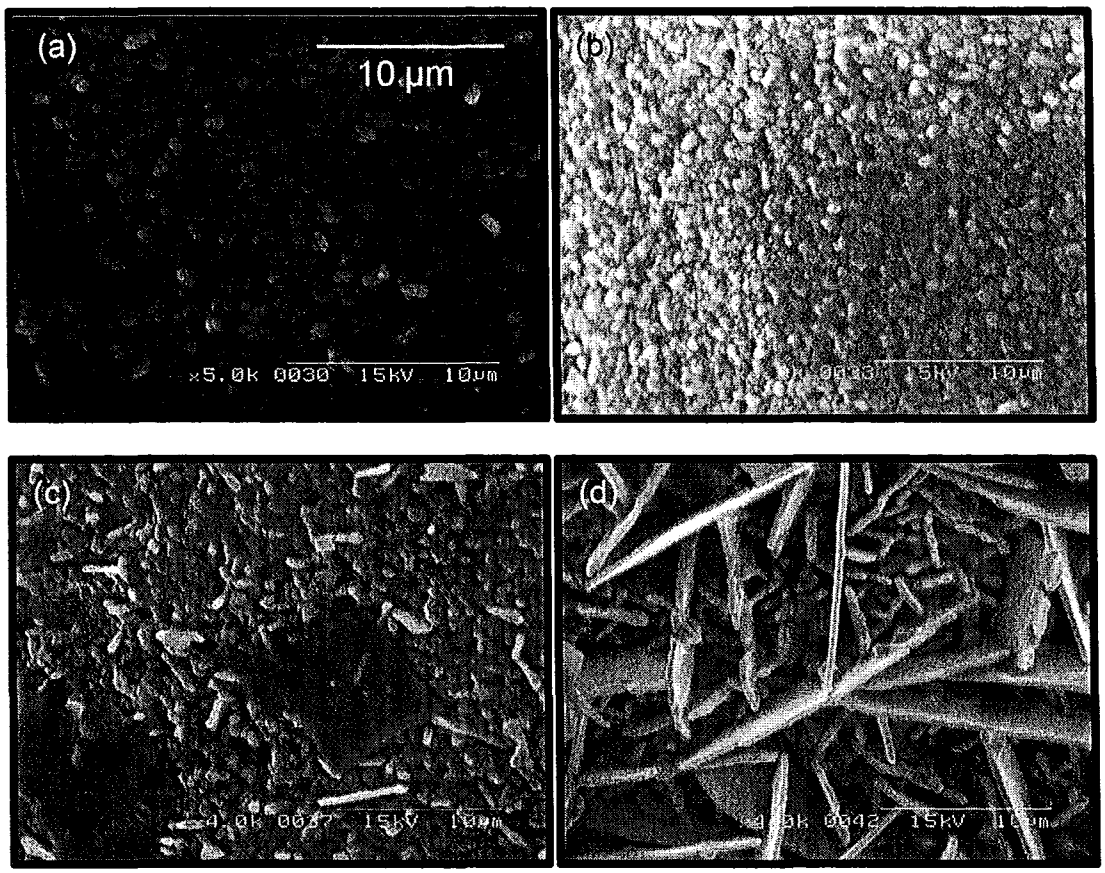

Figure 5.7 The side views of SEM pictures of silver chloride on silver wire grown in 1 M KCl against platinum wire with 1 cm spacing for 15 min when the cathodic potential was 0.2 V. The pictures indicate the anodic potential _ frequency in which the transition from nansheet structure into globular structure occurs (a) 1.5V_5Hz (b) 2V_5kHz (c) 3V_5MHz (d) 2V_12.5 MHz (The scale bar in the top right corner of the composite image applies to all individual images.)

wire for 15 minutes. The frequency was increased up to the level at which the nanosheet structure is converted into the globular structure. The SEM pictures in Figure 5.7 demonstrates the significant effect of the anodic potential on growth of the nanosheet. The frequency at which transition from the nanosheet structure into the globular structure increases accordingly. At 1.5 V anodic potential the transition occurs at frequency of 5 Hz (Figure 5.7 (a)) while at 2 V anodic potential it happens at 5 kHz (Figure 5.7 (b)).

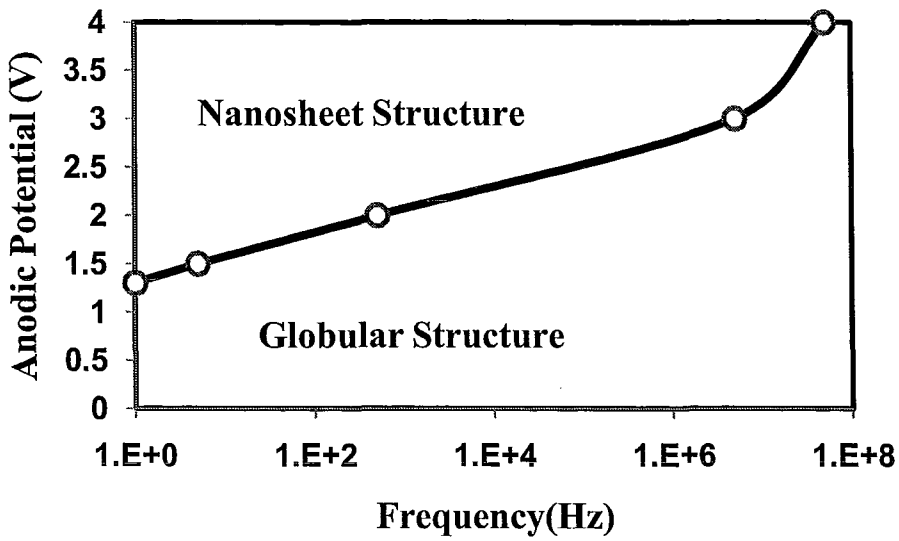

Figure 5.8 Schematic demonstration of anodic potential-frequency relationship and their effects on silver chloride morphology

Increasing the anodic potential to 3 V requires the least frequency of 5 MHz to create the globular structure (Figure 5.7 (c)). At 4 V anodic potential, the needed frequency to create the globular structure exceeds the maximum frequency which can be generated by AC power supply, e. g., 12.5 MHz and the AgCl has still nanosheet structure (Figure 5.7 (d)). Figure (5.8) is the schematic demonstration of the effect of the anodic potential and frequency on the silver chloride morphology.

In order to test effect of the magnitude of the cathodic potential on the electrodeposited silver chloride morphology, an asymmetric potential at a constant frequency of 0.5 Hz and an anodic potential of 2 V was applied in 1 M KCl against a platinum wire with 1 cm spacing. Increasing the applied cathodic potential from 1 V to 2V makes the AgCl surface smoother (Figure 5.9). Following this observation, the AgCl structure prepared by a cathodic voltage of 1.8 V (Figure 5.9(d)) is solely globular and

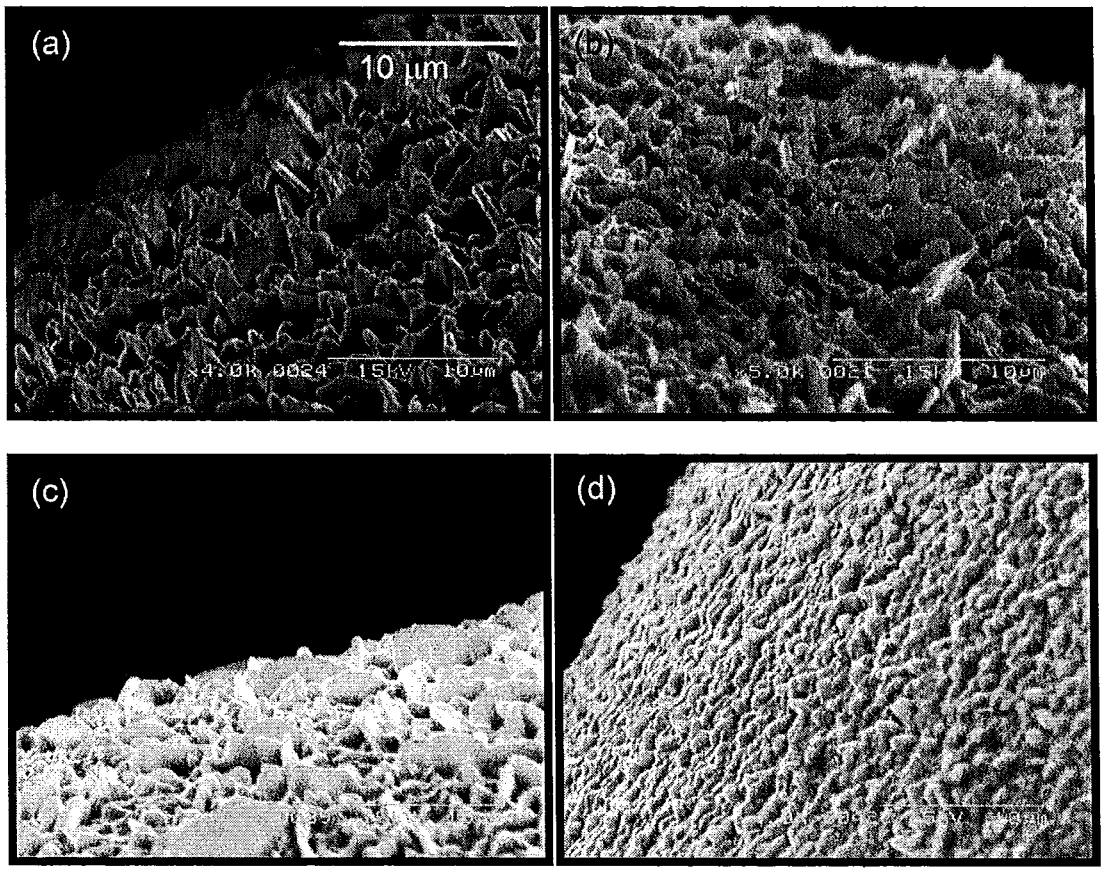

Figure 5.9 The side views of SEM pictures of silver chloride on silver wire grown in 1 M KCl against platinum wire with 1 cm spacing by applying constant anodic potential of 2 V and different cathodic potentials (V) at 0.5 Hz for 15 min, (a) 0.2 (b) 1 (c) 1.6 (d) 1.8. (The scale bar in the top right corner of the composite image applies to all individual images.)

grains are denser compared to that at 0.2 V (Figure 5.9(a)). In fact, an increment in the cathodic potential increases the side growth of the nanostructures which supports the globular structure growth.

(II) Effect of AgCl Morphology on Stability of Ag/AgCl Electrode

The stability of the potential of the reference electrodes is an important property in BioFET that can be affected by the morphology of the silver chloride, as previously

explained in chapters 2 and 3. In order to analyze the effect of the formation of nanosheet structures of AgCl on the stability of the reference electrode potential, an open-circuit test of bare Ag/AgCl electrodes, fabricated under both DC and AC conditions, were performed in 1 M KCl versus the commercial calomel reference electrode for 15 hours. Figure 5.10 shows the open-circuit potential measurement of the bare Ag/AgCl electrode prepared at (a) anodic DC potential of 2 V (b) anodic and cathodic potentials of 2 and 0.2 V, respectively with frequency of 0.5 Hz (c) anodic DC potential of 0.5 V (d) anodic and cathodic potentials of 2 and 0.2 V, respectively with frequency of 50 kHz in 15 min. Based on the definitions presented in section 5.1, a drift of 0.5 mV is obtained for the Ag/AgCl electrode with a nanosheet AgCl morphology (case (a) and (b)) whereas it is 7 mV (case c) and 2 mV (case d) for the Ag/AgCl electrode with a globular AgCl morphology in 15 hours. In brief, Ag/AgCl electrode with nanosheet AgCl morphology (case (a) and (b)) provides more stable potential than the one with globular AgCl morphology (case (c) and (d)) prepared in both modes of DC and AC deposition. This achievement is in an agreement with the discussion explained in section 3.3 that structure with higher surface area leads to more stable potential. In fact, in this kind of experiments the noise is typically imposed by external sources such as charged particles in the ambient air, the semiconductor parameter analyzer, and the commercial reference electrode instability. This noise appears as a current which is imposed by the external sources which can be dramatically reduced by increasing the surface area of the silver chloride.

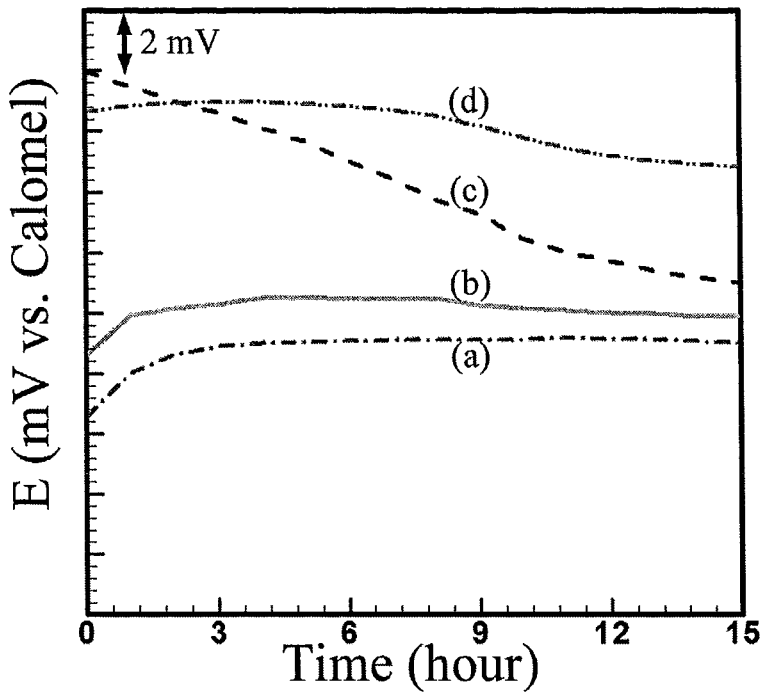

Figure 5.10 Stability of the bare silver/silver chloride electrode grown by (a) 2 V DC (b) 2 V (anodic)_0.2 V (cathodic) at 0.5 Hz (c) 0.5 V DC (d) 2 V (anodic)_0.2 V (cathodic) at 50 kHz for 15 min against the standard calomel electrode in 1 M KCl.

(II) Mechanism of AgCl Structure Growth

It is known that the electrochemical deposition parameters such as temperature, applied potential, electrolyte concentration and time play key roles in controlling the morphology, especially its uniformity on the substrate. In this study, all of the electrodeposition experiments were performed at the same conditions, except for the anodic/cathodic potential and frequency. The growth of the nanosheets, then, should be attributed to the deposition potential/current density and frequency. In order to obtain the current density variation during the deposition, LabTracer software (Keithley company) was used to control and record the electrodeposition potential and current, respectively.

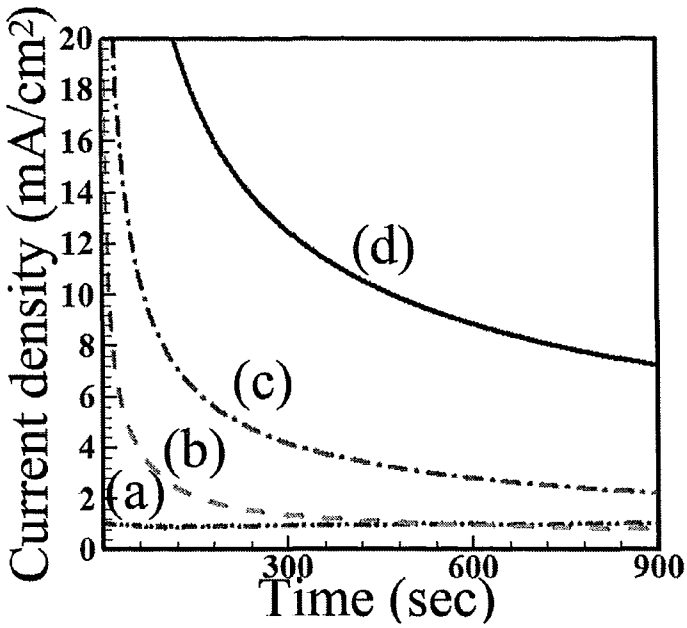

Figure 5.11 Deposition current density of silver chloride on silver wire versus time in DC mode in 1 M KCl against platinum electrode (a) 0.5 V (b) 1 V (c) 2 V (d) theoretical current density based on equation (2.23) (D_{Cl}=2.03×10^{-5} cm^2/s [Cussler 1997])

The electrodeposition of AgCl on Ag wire was performed in 1 M KCl against a platinum wire at 0.5, 1, and 2 V DC mode. Results, such as demonstrated in Figure 5.11 (a), indicate the constant current density of 1 mA/cm^2 at 0.5 V DC anodic potential. At 1 V applied bias, the current density starts at a high value of 20 mA/cm^2 and rapidly reduces to become constant (1 mA/cm^2) at around 5 minutes (Figure 5.11 (b)). A similar trend is found at 2 V anodic potential in which current density has initial value of ~100 mA/cm^2 and decreases rapidly and does not become stable within the deposition time (Figure 5.11 (c)). When the applied overpotential is small, the electrochemical reaction is kinetically controlled and the current remains constant, as given by equation (2.19). It should be noted that the resistance is approximately constant in this case due to the

imposition of slight current density and slow growth of the silver chloride layer. When the applied overpotential becomes higher, the concentration of reactants at the electrode surface becomes zero and the reaction becomes mass transfer controlled (equation (2.23)). The diffusion layer slowly starts increasing (equation (2.22)) and this leads to the drop in the current density, as shown in the model plotted in Figure 5.11 (d). In Figure 5.11 (d), the current density based on equation (2.23) was plotted to compare it against the experimental results. In this case, the following values were inserted in equation (2.23): $D_{Cl}=2.03\times10^{-5}$ cm^2/s [Cussler 1997], F=96486 C mol^{-1}, n=1, $C^*=1$, C=0. At 0.5 V, the reaction rate controlled deposition occurs. However, an increment in deposition potential will reduce concentration of chlorine at the electrode surface, and subsequently, mass transport phenomenon will become dominant. Also, at 1 V and 2 V DC anodic depositions, the current density has a similar trend to the theoretical graph based on the mass transport current density. It should be noted that the current density is very high and even after 5 minutes is not stabilized what indicates the resistance of AgCl layer can not be responsible for the trend of the current density.

We hypothesize that the mode of deposition is responsible for the morphology of electrodeposited AgCl. In fact, at a low anodic potential, all the nucleation sites receive the same flux of Cl^- ions that participates in the AgCl formation. Therefore, the AgCl grows at the same rate without any preferential growth. On the other hand, a high anodic potential transforms the mode of deposition from reaction rate into mass transport. In the mass transport mode, Cl^- is exhausted rapidly at the electrode surface and, therefore, its concentration decreases substantially in the vicinity of the Ag wire (assumed to be zero).

In this case, diffusion is responsible for delivering chlorine to the electrode surface. As seen in equation (2.22), diffusion is a function of the bulk Cl^- concentration and the stagnant layer in which the former is constant and the latter increases as time elapses (assuming zero concentration of Cl^- at the electrode surface). It should be noted that the stagnant layer has uniform peripheral growth respect to the electrode surface. In the case of nanostructure growth on the Ag surface, the denominator in equation (2.22) will increase or decrease since the distance between reaction location (tip of the structure) and the bulk solution is not a stagnant layer any more. Assuming the height of silver chloride to be H, then equation (2.22) can be rewritten in the following format:

$$\left(\frac{\partial C}{\partial z}\right)_{0\leq z\leq \delta - H} = \frac{C^* - C(z = H)}{\delta - H} \tag{5.2}$$

Among the nucleation sites, those which are taller will receive more chlorine during deposition due to the higher rate of Cl^- transport based on equation (5.2) (Figure 5.12). Therefore, in the mass transfer control, initial small difference in nucleation growth rates rapidly leads to accelerated growth of the nanosheets in the direction of the concentration gradient.

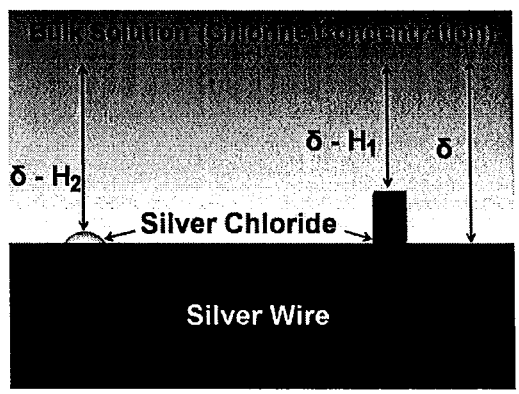

Figure 5.12 Silver chloride growth on silver wire.

The effect of frequency could be explained by the effect of interruption in chlorine accumulation at the silver wire surface. Applying high AC anodic voltage (2 V) converts silver into silver chloride in the non-steady state mass transport mode. In this case, similar to the high DC voltage deposition, the concentration of chlorine in the electrode vicinity is zero because of the fast chlorine consumption (section 2.3.2 part (III)). As explained before, in the mass transport mode of deposition, growth of nucleation sites of nanosheet structure is more favorable than other sites. Therefore, as long as the anodic potential is applied, the nanosheet height increases. Based on equation (2.21), the stagnant layer thickness increases during the deposition time. Once the deposition stops and becomes cathodic, it becomes constant. It should be noted that the stagnant layer does not decrease during imposition of a cathodic potential since in this experiment, it is less than the reverse reaction activation energy (as will be shown in the next paragraph). In this case, the chlorine concentration at the electrode surface increases and will be no longer zero. Therefore, at the next anodic deposition step, deposition of silver chloride starts with the reaction rate mode. Once the concentration of chlorine becomes zero, similar to high anodic deposition, the mass transport mode becomes dominant again. As the frequency increases, the anodic deposition duration becomes shorter and, therefore, the mass transport mode establishes for shorter period of time respect to the low-frequency deposition. In this case, the entire silver chloride structure will have uniform access to Cl^-. At high frequency, the silver chloride layer grows uniformly and at the same pace everywhere.

It has been shown ([Cheema 1971]) that the reverse reaction activation energy for reaction (2.28) is about -0.44 eV. As a result, the morphology does not vary significantly with cathodic voltages up to -0.5 in the AC mode. From -0.5 onwards, the structure becomes smoother (Figure 5.9). As seen in the preceding paragraph, the taller nanostructure likely has a faster growth. However, when backward reaction happens, they become smaller and finer. At higher cathodic voltage, the reverse reaction dominates, and as a result, the reverse current density converts the tall nanosheet into the globular structure.

5.2.2 CHARACTERIZATION OF THE MICROFLUIDIC REFERENCE ELECTRODE

For the rest of experiments, the Ag/AgCl electrode was prepared by anodic potential of 2V, cathodic potential of -0.2 V, and frequency of 0.5 Hz for 15 min. These conditions generate the silver chloride layer with the nanosheet structure which improves the stability substantially as demonstrated in section 5.2.1. Also, use of AC deposition allows the control of the silver chloride morphology by the frequency. To investigate the effect of membrane pore size on effusion of the internal solution, open-circuit potential measurement of the microfluidic reference electrode with stationary liquid junction was performed in PBS while the open area of the membrane was constant (500μm x 500μm). Less effusion of chlorine keeps the internal chlorine concentration constant and, then, the electrode potential remains stable. Similarly, and for the same purpose, open-circuit potential measurements of the reference electrode with various open areas of the

membrane and the most suitable pore size, obtained in the previous experiment, was conducted. In addition, effect of the rate and direction of the flow of the internal solution in the microchannel on the reference electrode potential reproducibility was studied. In this case, for each flowrate, a stability test was performed for 5 hours to ensure establishment of steady-state condition. Long term stability test of the microfluidic reference electrode (with optimum pore size and flowrate) in different configurations were performed to study the effect of configuration on the reference electrode's stability and lifetime. Furthermore, the effect of pH of the external solution was tested by adding acetic acid into the external solution to decrease the pH. Also, in order to investigate the effect of the chlorine concentration of the external solution, stationary liquid junction microfluidic reference electrode was tested in KCl solution with various concentrations (10mM-3M). In all the experiments, discussed here, three samples were tested and the best results were plotted.

(I) Effect of Interface Membrane Pore Size on Potential Stability

Open-circuit potential measurements results of the microfluidic reference electrode with different membrane pore size are presented in Figure 5.13. The membrane with pore size variation from 10 to 100 nm was assembled with a reference electrode using the process introduced in section 4.6. The open area of the membrane was kept the same in all experiments (500 μm x 500 μm). The purpose of this experiment is to investigate the effect of membrane pore size on effusion of internal Cl^-. Less effusion of Cl^- keeps the internal Cl^- concentration constant and then, the electrode potential remains stable.

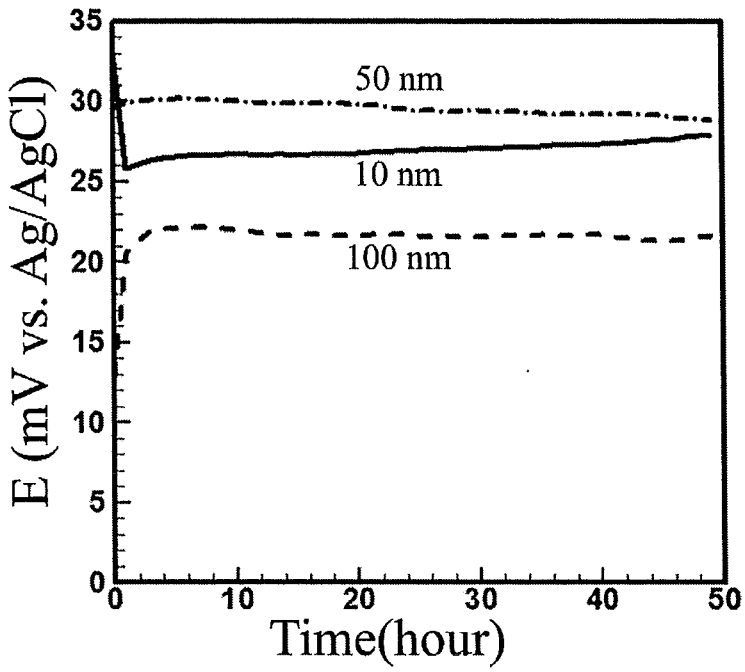

Figure 5.13 Stability test of microfluidic reference electrode with stationary liquid junction and different membrane pore size in PBS 10X.

As demonstrated in Figure 5.13, there is no significant variation in the stability (~30 μV, as defined in equation (5.1)) of the reference electrode potential in a 50 hour period of test, although the drift using 10 nm pore size (~1.8 mV) is slightly more than the other two pore sizes (~1.5 mV). Hence, the preference is given to the largest pore size that prevents the interface from clogging, e.g., 100 nm.

(II) Effect of Interface Membrane Open Area on Potential Stability

In the next set of experiments, the effect of the open area of the membrane with 100 nm pore size on electrode potential stability was studied. Similar to the pore size study, a smaller open area of the membrane is expected to restrict effusion of the internal chlorine. However, open-circuit potential measurements of the reference electrode with

open area of 300 μm x 300 μm, 500 μm x 500 μm, and 700 μm x 700 μm do not demonstrate noticeable difference in terms of stability, which are 30, 30, and 23 μV, respectively (Figure 5.14). In terms of drift, the 500 μm x 500 μm and 700 μm x 700 μm areas showed slightly less drift (0.5 mV) respect to 300 μm x 300 μm area (0.8 mV) over 50 hours. Since this difference is not significant, it can be neglected. In the rest of experiments, the microfluidic reference electrode has 100 nm pore size membrane with open area of 500μm x 500μm.

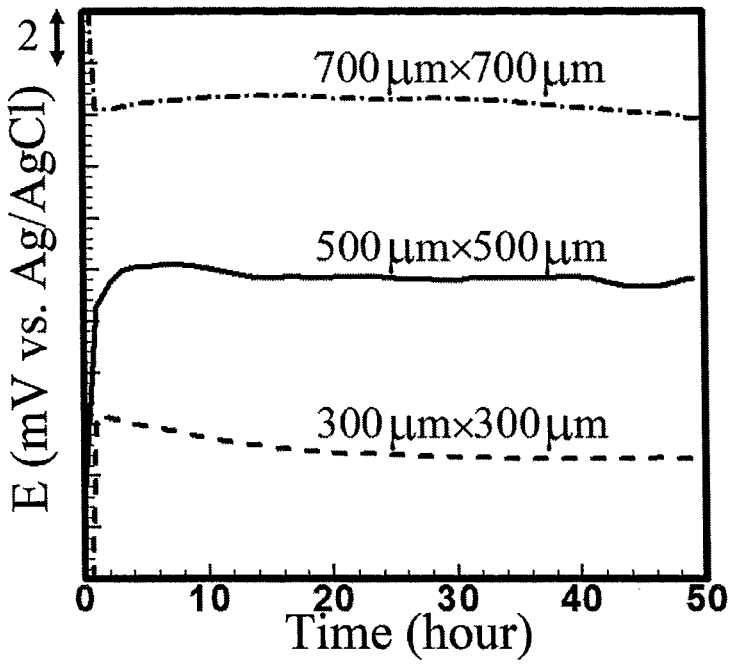

Figure 5.14 Stability test of microfluidic reference electrode with stationary liquid junction and different open area of 100 nm membrane in PBS 10X.

(III) Determination of Optimum Flowrate in Reference Electrodes with Flow of Internal Solution and Free-Diffusion Liquid Junction

In order to replenish the internal solution and improve the reference electrode potential stability, the reference electrode configuration with flow of internal solution was

used. The optimum flowrate and direction of the internal solution in the microchannel was determined by observing effect of the internal flow on the microfluidic reference electrode stability (Figure 5.15). As the results show, a high flowrate (>1μL/min), in both modes of flow of the internal solution inside the microchannel, increases the irreproducibility of the reference electrode potential (~2-3 mV) compared to the stationary liquid junction reference electrode configuration. In fact, the higher flowrate results in a higher velocity in the internal solution which potentially can detach the AgCl layer from the electrode's surface. Upon detachment of the silver chloride layer, the underneath silver will be suddenly exposed to solution suddenly on which some other reactions might proceed. Also, the potential reproducibility is not affected by the direction of the internal solution flow.

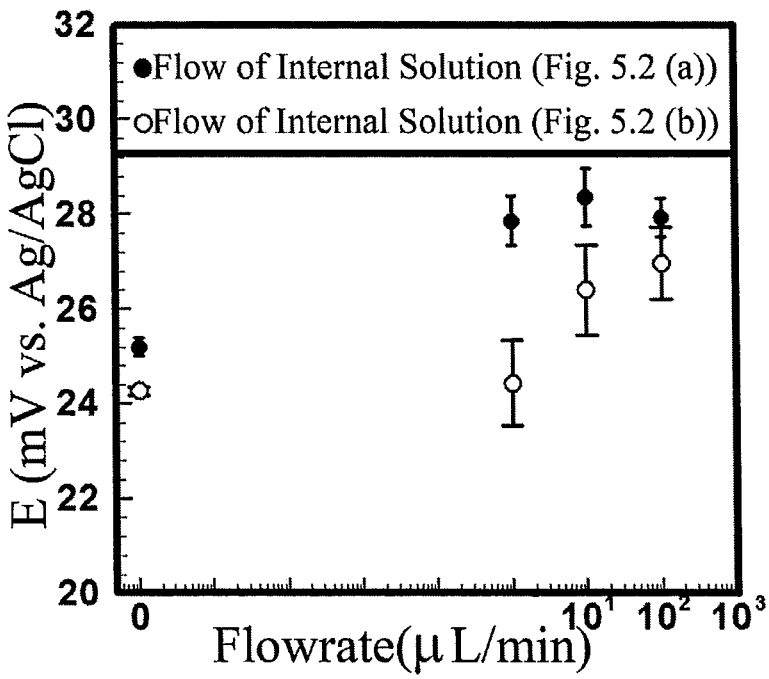

Figure 5.15 Effect of flow of internal solution in microchannel on microfluidic reference electrode stability.

Therefore, for further open-circuit potential tests of the reference electrode with a flow of internal solution in the microchannel, the flowrate was set to be 1μL/min. Also, to be consistent in the experiments, the mode where the fresh solution arrives at the porous interface before reaching the Ag/AgCl wire (Figure 5.2 (a)) was chosen in the reference electrode with an internal solution flow configuration. For the free-diffusion liquid junction test, the flowrate was set to be 2μL/hour to prevent the external solution from contamination by the internal solution. This flowrate corresponds to 50 μm/sec velocity of KCl inside the pores which is still capable of offsetting the liquid junction effect.

(IV) Effect of Reference Electrodes Configuration on Its Potential Stability

The microfluidic reference electrode (regardless of its configuration) can extend the life time of the bare Ag/AgCl electrode from 63 hours to at least 100 hours (Figure 5.16). The following numeric values for stability and lifetime are obtained using equation 5.1. Stability test of the bare silver/silver chloride wire shows 2.2 mV drift over 63 hours lifetime at which the stability is 34 μV. For the case of microfluidic reference electrode with stationary liquid junction (see Figure 5.1 (a)), the stability is found to be 45 μV over 100 hours with 5 mV drift. Furthermore, a flow of 1 M KCl through the microchannel (1 μL/min) improves the reference electrode performance in such a way that the drift and stability are 1.7 mV and 27 μV, respectively over 100 hours (Figure 5.2(a)). In the final case, the flowrate across the membrane was set to be 2 μL/hr (see Figure 5.1 (b)) which results in 1 mV drift and 40μV stability over 100 hours (see Figure 5.16). Therefore, in order to improve the stability and reduce the drift of the

microfluidic reference electrode potential, a flow of internal solution through either the microchannel or across the membrane is essential. As explained in chapter 3, the liquid junction potential effect vanishes with a flow of internal solution across the membrane. Thereby, concern of dynamic and static deviations in the reference electrode potential is mostly alleviated (section 3.3). Furthermore, flow of the internal solution replenishes the surrounding solution of the electrode continuously, which enables the electrode to work consistently during the test. In the case of a flow of internal solution in the microchannel, the internal solution concentration can be retained; however, the effect of liquid junction increases the instability because of the diffusion of the external solution into the junction. Finally, a stationary liquid junction reference electrode can offer more stable potential than a bare electrode; however, its drift is higher than other configurations.

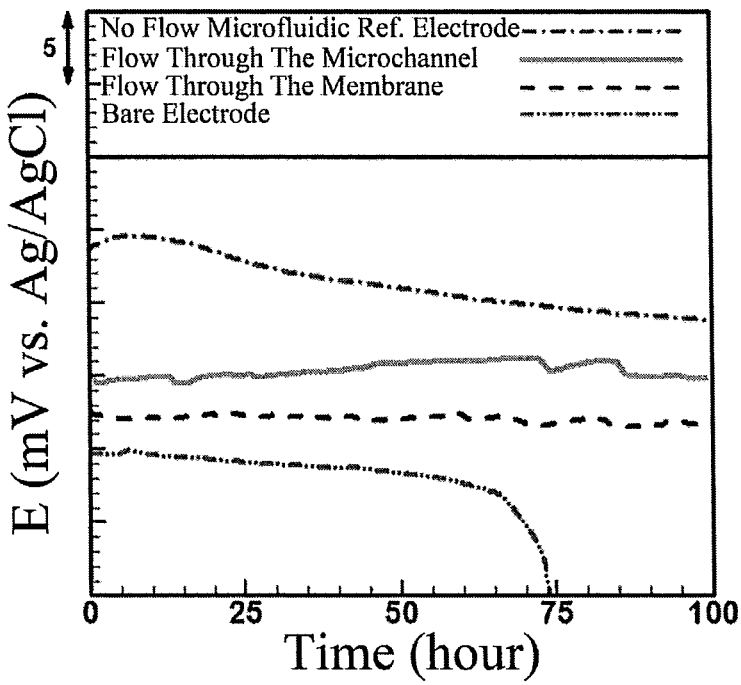

Figure 5.16 Open-circuit potential measurement between reference electrodes and commercial Ag/AgCl in PBS.

The drift can be attributed to conversion of the AgCl into Ag^+ and Cl^- which increases the concentration of chlorine at the vicinity of the electrode due to the small volume of microchannel. An increase in the internal solution concentration results in potential creep towards the zero axis (equation 2.29) because of the reduction in potential difference between the microfluidic reference electrode and the commercial Ag/AgCl electrode.

(V) Effect of External Solution pH and Chlorine Concentration on Reference Electrode Potential

As seen in Figure 5.17, the bare Ag/AgCl electrode responds to the variation of chlorine in the external solution based on Nernst equation (equation 2.29). In contrast, a microfabricated reference electrode with stationary liquid junction is insensitive to the pH. It can be explained by considering nanoporous membrane as a barrier for the external chlorine to diffuse into the internal solution. Similarly, and for the same reason, the microfluidic reference electrode does not demonstrate any sensitivity to the pH of the external solution although it can not be tested in a basic solution since operation of the membrane is restricted to the pH's in the range of 4-8 (Figure 5.18). The bare Ag/AgCl electrode was tested in the solution with various pH values. Figure 5.18 indicates that although the reproducibility of the bare electrode potential is not comparable with the microfluidic reference electrode in various pH, however, the potential remains quite stable. This result is in agreement with equation (2.29) since the chlorine concentration will not vary with pH and, therefore, the electrochemical potential remains constant for bare Ag/AgCl electrode.

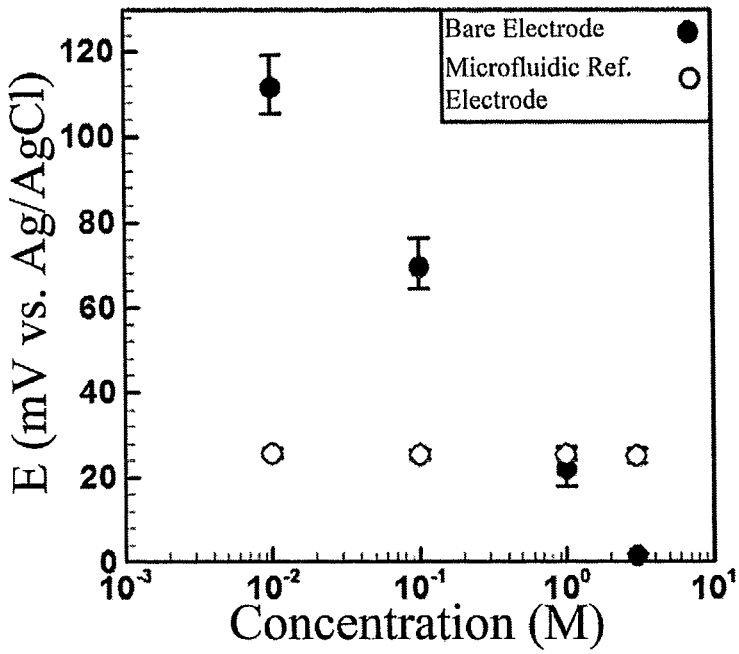

Figure 5.17 Effect of chlorine concentration of external solution on microfluidic reference electrode (stationary liquid junction) and bare electrode stability in KCl against commercial Ag/AgCl.

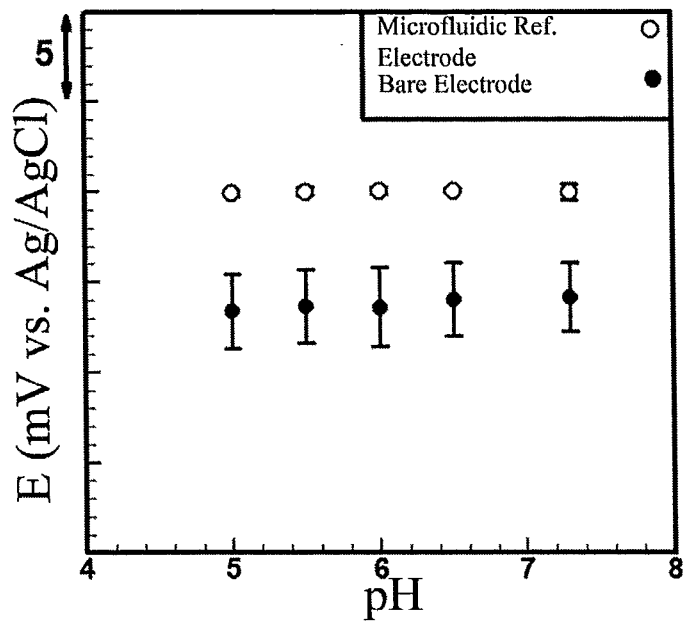

Figure 5.18 Effect of pH of external solution on microfluidic reference electrode (stationary liquid junction) and bare electrode stability in PBS against commercial Ag/AgCl.

5.3 SUMMARY

In conclusion, the effect of silver chloride deposition conditions on silver wire was studied and it was found that the anodic electrodeposition of silver chloride at a high anodic potential (>0.5) can generate nanosheet silver chloride structure as opposed to conventional globular structure. The nanosheet structure was found to transform into the globular structure by applying high frequency (50 kHz) asymmetric electrodeposition with high anodic potential (2V). The nanosheet structure was found to improve the Ag/AgCl electrode potential stability significantly in comparison with the globular structure. Also, the effect of the membrane's pore size and open area on the reference electrode potential stability was studied, but no significant effect was observed. Open-circuit potential measurement of the bare Ag/AgCl and three configurations of the microfluidic reference electrode including stationary liquid junction, flow of internal solution inside the microchannel, and free-diffusion liquid junction were performed. It was demonstrated that the microfluidic reference electrode with different configurations have longer stable lifetime (100 hours) in comparison to the bare Ag/AgCl electrode (63 hours), among which, the free-diffusion liquid junction offers stable potential (40 μV) with the least drift (1 mV). Finally, the effect of the external solution's pH and chlorine on both bare and microfluidic reference electrodes was investigated. No sensitivity of the microfluidic reference electrode to pH and chlorine variation was observed whereas the bare Ag/AgCl electrode potential demonstrated several mV of instability.

Chapter 6

CONTRIBUTIONS AND FUTURE WORK

6.1 CONTRIBUTIONS

The contributions, which were made in this thesis research work, can be divided into two main categories. First, a novel electrodeposition of silver chloride on silver wire produces silver chloride with nanosheet structure which makes the Ag/AgCl electrode potential more stable than conventional globular structure. Second, the free-diffusion liquid junction configuration was incorporated with the microfluidic Ag/AgCl reference electrode which substantially improves its stability and lifetime in comparison with the other configurations.

6.1.1 GROWTH OF NANOSHEET SILVER CHLORIDE

A high DC voltage (>0.7V) was used to deposit silver chloride on silver wire anodically. The resulting morphology of silver chloride was found to have nanosheet structure as opposed to conventional silver chloride globular structure morphology. In addition, a novel asymmetric electrodeposition was used to grow and control the nanosheet structure. It was shown that at an anodic potential of 2 V and a cathodic potential of -0.2 V deposition, by increasing the frequency and the cathodic potential, the nanosheet silver chloride turns into the globular structure at 50 Hz and -1.6 V, respectively.

A Ag/AgCl electrode with nanosheet silver chloride structure showed more stable potential in comparison to Ag/AgCl electrode with conventional silver chloride structure (globular structure), regardless of the electrodeposition conditions. The former showed <0.5 mV drift and the latter showed 2-7 mV drift over 15 hours of operation in 1 M KCl. This improvement was attributed to the reduction in the local current density. In fact, an increase in the surface area of the silver chloride results in less current density at electrode/electrolyte interface which stabilizes the electrode potential. It was concluded that the nanosheet silver chloride improves the stability of reference electrodes and can be used for the next generation of reference electrodes which are used to measure or impose potential in solutions.

6.1.2 MICROFLUIDIC REFERENCE ELECTRODE

As explained in chapter 2, reference electrodes, which have been microfabricated so far, have several issues such as short lifetime and instability of the electrode potential. To overcome this problem, a protective polymer layer on the electrode has been used to encapsulate the electrode. The electrode is in a reservoir which has liquid junction as interface to the external solution. However, the liquid junction itself is one of the sources of the potential instability in these reference electrodes.

To overcome the effect of the liquid junction and improve the stability and lifetime of these reference electrodes, this thesis research is focussed on a microfluidic silver/silver chloride reference electrode with a precisely defined interface (500 μm x 500 μm) and 1 M KCl as the internal solution. In terms of stability and

lifetime, it was shown that the flow of the internal solution across the membrane can improve both stability and drift to 40 μV and 1 mV, respectively, over 100 hours of operation. This is more desirable for use in BioFET than other configurations. It was also observed that the liquid junction microfluidic reference electrode does not show any sensitivity to pH and chlorine concentration of the external solution.

In conclusion, three configurations of a microfluidic reference electrode were tested. It was demonstrated that all of them have stable potential over 100 hour which are comparable with the previous reports. Finally, microfluidic reference electrode with the free-diffusion liquid junction offers a stable potential with significantly reduced drift over operation time distinguishing this thesis from the previous works.

6.2 FUTURE WORK

Performance of the microfluidic reference electrode that was designed and fabricated in this thesis can be improved in several aspects which are listed here:

DESIGN AND FABRICATION

- The device can be further miniaturized by reducing the length of the microchannel, as it does not affect the overall performance of the device.
- In this research, integration of the bare electrode into the microchannel was performed manually by penetrating a needle into the PDMS microchannel and passing the electrode through the needle into the microchannel. There is a potential risk to wipe off the silver chloride

coating layer. The possible improvement can be performed by placing the electrode into the microchannel during PDMS casting process. However, precautions should be taken to avoid any contact between silver chloride coating layer and liquid PDMS.

TEST SET UP AND EXPERIMENTAL DESIGNS

- The pre-treatment process was too time consuming, especially for the free-diffusion liquid junction microfluidic reference electrode. Optimization of this procedure is one of the possible future works that shortens the microfluidic reference electrode preparation time.
- The effect of the flow of the external solution on the fabricated reference electrodes can be investigated. It may be found useful for its application in BioFET where there is a flow of solution in BioFET's reservoirs to introduce the DNA molecules. It can be performed by designing a proper container to drive the external solution into and out of the test setup.

DEVICE PERFORMANCE IMPROVEMENT

- A higher mass of silver chloride can be deposited onto the silver wire in a longer period of deposition, which can extend lifetime of the reference electrode. However, a thick silver chloride layer can increase the possibility of the instability. Optimization of silver chloride deposition on silver wire is one of the possible future work.

- As mentioned before, some groups used some polymers as protective layer on electrode. Incorporation of this technique with free-diffusion liquid junction microfluidic reference electrode is one of the possible modifications. Agar gel has been extensively used as porous protective layer which can be pasted on silver chloride region of the Ag/AgCl electrode. The rest of fabrication process would be the same as the current thesis research. It should be noted that placing agar gel on the membrane may increase the effect of liquid junction and also may be detached by flow of the internal solution through the membrane.

References

[Amadi 1991] Amadi, S. A., et al., "Electrochemical mass transport sensor to study agitation in electroplating processes", Applied Electrochemistry, 21, pp. 1114-1119, 1991.

[Bakker 2002] Bakker, E., et al., "Electrochemical sensors", Analytical Chemistry, 74, pp. 2781-2800, 2002.

[Bergveld 1970] Bergveld, P., "Development of an ion-sensitive solid-state device for neurophysiological measurements," IEEE Transactions on Biomedical Engineering, BME-17, pp. 70-71, 1970.

[Bard 1962] Bard, A. J., "Inhibition of hydrogen ion reduction at a platinum electrode by tin hydrous oxide film formation", Electroanalytical Chemistry, 3, pp. 117-125, 1962.

[Brad 1980] Bard, A. J., Faulkner, L. R., "Electrochemical methods: fundamentals and applications", John Wiley and Sons Inc., 1980.

[Bashir 2004] Bashir, R., "BioMEMS: state-of-the-art in detection, opportunities and prospects", Advanced Drug Delivery Reviews, 56, pp. 1565-1586, 2004.

[Beck 1984] Beck, T. R., et al., "Conductivity of anodic silver chloride during formation", Electrochemical Society: Electrochemical Science and Technology, 131, pp. 89-93, 1984.

[Bejamin 2005] Benjamin, H., et al., "A planar micro-sensor for bio-impedance measurements", Sensors and Actuators B, 111-112, pp. 430-435, 2005.

[Bockris 1964] Bockris, J. O'M., et al., "The anodic formation of calomel films on mercury electrodes an ellipsometric-galvanostatic study", Proceeding Royal Society of London A, 279, pp. 327-345, 1964.

[Brezinski 1983] Brezinski, D. P., "Kinetic, static and stirring errors of liquid junction reference electrodes", Analyst, 108, pp. 425-442, 1983.

[Buck 2001] Buck, R. P., et al., "Tracing the history of selective ion sensors", Analytical Chemistry, 97, pp. 88-100, 2001.

[Cussler 1997] Cussler, E. L., "Diffusion: mass transfer in fluid systems", Cambridge University Press, 2 edition, 1997.

[Czaban 1976] Czaban, J. D., et al., "Glass microelectrode probes for routine ph measurements", Analytical Chemistry, 48, pp. 277-281, 1976.

[Dohner 1986] Dohner, R. E., et al., "Reference electrode with free-flowing free-diffusion liquid junction", Analytical Chemistry, 58, pp. 2585-2589, 1986.

[Duan 2001] Duan, Y. Y., et al., "Potential applications of a small and high surface area platinum electrode as an implanted impedance bio-sensor or recording electrode", Proceedings of Society of Photographic Instrumentation Engineers, 4235, pp. 145-153, 2001.

[Feng 2003] Feng, R., et al., "Influence of processing conditions on the thermal and mechanical properties of su8 negative photoresist coatings", Micromechanical and Microengineering, 13, pp. 80-88, 2003.

[Franklin 2005] Franklin, R. K., et al, "Iridium oxide reference electrodes for neurochemical sensing with MEMS microelectrode arrays," IEEE Sensors, pp. 1400-1403, 2005.

[Fu 2003] Fu, P. F., et al., "Polypropylene-polysiloxane block copolymers via hydrosilylation of monovinylidene capped isotactic polypropylene", ACS Polymer Preprint., 44, pp. 1014-1015, 2003.

[Gabig 2001] Gabig, M., et al., "An introduction to DNA chips: principles, technology, applications and analysis", Acta Biochimica Polonica, 48, pp. 615-622, 2001.

[Garbett 1975] Garbett, K., et al., "Capillary tip reference electrode based on a glass syringe [for metal surface corrosion measurement]", Laboratory Practice, 24, p. 248, April 1975.

[Gibbs 1899] Gibbs, J. W., "Collected works", Longman, NewYork, volume 1, 1899.

[Giner 1964] Giner, J., "A practical reference electrode," Journal of the Electrochemical Society, 111, pp. 376-377, 1964

[Guth 2009] Guth, U., et al., "Recent developments in electrochemical sensor application and technology-a review", Measurement Science and Technology, 20, pp. 13-26, 2009.

[Heller 2002] Heller, M. J., "DNA microarray technology: devices, systems, and applications", Annual Review Biomedical Engineering, 4, pp. 129-153, 2002.

[Hleli 2003] Hleli, S., et al., "Impedance spectroscopy technique for DNA hybridization", Sensors, 3, pp. 472-479, 2003.

[Huang 2002] Huang, I-Y, et al., "Fabrication and characterization of a new planar solid-state reference electrode for ISFET sensors", Thin Solid Films, 406, pp. 255-261, 2002.

[Illingworth 1981] Illingworth, J. A., "A common source of error in pH measurements", Biochemical, 195, pp. 259-262, 1981.

[Ives 1961] Ives, D. J. G., Janz, G. J., "Reference electrodes: theory and practice", Academic Press, 1961.

[Janz 1963] Janz, G. J., et al., "Silver/silver chloride electrodes", Annals New York Academy of Sciences, pp. 210-221, 1963.

[Jin 2003] Jin, X., et al., "The electrochemical formation and reduction of a thick AgCl deposition layer on a silver substrate", Electroanalytical Chemistry, 542, pp. 85-96, 2003.

[Katan 1974] Katan, T., et al., "Silver/silver chloride electrodes: surface morphology on charging and discharging", Electrochemical Society: Electrochemical Science and Technology, 121, pp. 757-765, 1974.

[Kim 2004] Kim, H. R., "Enhancement of physical and chemical properties of thin film Ag/AgCl reference electrode using a Ni buffer layer," Sensors and Actuators B, 97, pp. 348-354, 2004.

[Kim 2006] Kim, S. K., et al., "A miniaturized electrochemical system with a novel polyelectrolyte reference electrode and its application to thin layer electroanalysis", Sensors and Actuators B, 115, pp. 212-219, 2006.

[Kitade 2005] Kitade, T., et al., "Needle-type ultra micro silver/silver chloride reference electrode for use in micro-electrochemistry", Analytical Sciences, 21, pp. 907-912, 2005.

[Koch 1999] Koch, S., et al., "Protein detection with a novel ISFET-based zeta potential analyzer", Biosensors and Bioelectronics, 14, pp. 413-421, 1999.

[Kulys 1993] Kulys J., et al., "The preparation in situ of a silver-silver chloride reference electrode", Electroanalysis, 6, pp. 945-952, 1994.

[Kunimatsu 2005] Kunimatsu, M., et al., "Microtubular hydrogen electrode, a reference electrode for electrochemical analyses", Electrochemical Society, 152, pp. E161-E166, 2005.

[Kwon 2007] Kwon, N-H., "An all-solid-state reference electrode based on the layer-by-layer polyumer coating ," Analyst, 132, pp. 906-912, 2007.

[Long 2003] Long, Y. T., "AC impedance spectroscopy of native DNA and M-DNA", Biophysical, 84, pp. 3218-3225, 2003.

[Maminska 2006] Maminska, R., et al., "All-solid-state miniaturised planar reference electrodes based on ionic liquids," Sensors and Actuators B, 115, pp. 552-557, 2006.

[Martinoia 2004] Martinoia, S., et al., "ISFET-neuron junction: circuit models and extracellular signal simulations", Biosensors and Bioelectronics, 19, pp. 1487-1496, 2004.

[McDonald 2002] McDonald, J. C., et al., "Poly(dimethylsiloxane) as a material for fabricating microfluidic devices", 35, pp. 491-499, 2002.

[McGill 1978] McGill, I. R., et al., "A novel reference electrode arrangement for high temperature polarisation studies", Corrosion Science, 18, pp. 257-259, 1978.

[Moussy 1999] Moussy, F., et al., "Prevention of the rapid degradation of subcutaneously implanted Ag/AgCl reference electrodes using polymer coatings," Analytical Chemistry, 66, pp. 674-679, 1999.

[Nagy 1997] Nagy, K., et al., "Promising new solid-state reference electrode", Electrochemical Society, 144, pp. L1-L2, 1997.

[Nann 2000] Nann, T., et al., "A new dynamic hydrogen reference electrode for applications in thin-film sensor systems", Sensors and Actuators B, 70, pp. 188-195, 2000.

[Niedermeyer 2005] Niedermeyer, E., Lopes da Silva, F. H., "Electroencephalography: basic principles, clinical applications, and related fields", Lippincott Williams & Wilkins, 2005.

[Nolan 1997] Nolan, M. A., et al., "Fabrication and characterization of a solid state reference electrode for electroanalysis of natural waters with ultramicroelectrodes," Analytical Chemistry, 69, pp. 1244-1247, 1997.

[Offenhausser 2001] Offenhausser, A., et al., "Cell-transistor hybrid systems and their potential applications", Trends in Biotechnology, 19, pp. 62-67, 2001.

[Okahata 1992] Okahata, Y., et al., "Hybridization of nucleic acids immobilized on a quartz crystal microbalance", Journal of American Chemical Society, 114, pp. 8299-8300, 1992.

[Park 2003] Park, S-I, "Application of a new Cl-plasma-treated Ag/AgCl reference electrode to micromachined glucose sensor," IEEE Sensors Journal, 3, pp. 267-272, 2003.

[Park 2008] Park, K. M., et al., "BioFET sensor for detection of albumin in urine", Electronics Letters, 44, pp. 185-U7, 2008.

[Pedrotti 1996] Pedrotti, J. J., et al., "Miniaturized reference electrodes with microporous polymer junctions", Electroanalysis, 8, pp. 673-675, 1996.

[Peters 1997] Peters, G., "A reference electrode with free-diffusion liquid junction for electrochemical measurements under changing pressure conditions", Analytical Chemistry, 69, pp. 2362-2366, 1997.

[Polk 2006] Polk, B. J., et al., "Ag/AgCl microelectrodes with improved stability for microfluidics", Sensors and Actuators B, 114, pp. 239–247, 2006.

[Roberge 2000] Roberge, P. R., "Handbook of corrosion engineering", McGraw-Hill, 1999.

[Saheb 2006] Saheb, A. et al., "Reference electrode for ionic liquids", Electroanalysis, 18, pp. 405-409, 2006.

[Sakata 2005] Sakata, T., et al., "DNA analysis chip based on field-effect transistors", Japanese Journal of Applied Physics, 44, pp. 2854-2859, 2005.

[Salle 1929] Salle, A. J., "A micro electrode and vessel for the determination of the hydrogen ion concentration of blood media, whole blood, and other biological fluids", Biological Chemistry, 83, pp. 765-772, 1929.

[Satyanarayana 2005] Satyanarayana, S., et al., "Stamp-and-stick room-temperature bonding technique for microdevices", Microelectromechanical Systems, 14, pp. 392-399, 2005.

[Savinell 1981] Savinell, R. F., et al., "Miniature glass ph electrode with nonaqueous internal reference solution", Analytical Chemistry, 53, pp. 552-554, 1981.

[Schöning 2002] Schöning, M. J., et al., "Recent advances in biologically sensitive field-effect transistors (BioFETs)", Analyst, 127, pp. 1137-1151, 2002.

[Selvaganapathy 2003] Selvaganapathy, P. R., et al., "Recent progress in microfluidic devices for nucleic acid and antibody assays", Proceedings of the IEEE, 91, pp. 954-975, 2003.

[Severinghaus 1958] Severinghaus, J. W., et al., "Electrodes for blood pO2, and pCO_2, determination", Applied Physiology, 13, pp. 515-520, 1958.

[Sevilla 1994] Sevilla, F., et al., "A bio-FET sensor for lactose based on co-immobilized β-galactosidasel glucose dehydrogenase", Biosensors & Bioelectronics, 9, pp. 275-281, 1994.

[Shibata 1977] Shibata, M., et al., "Miniature calomel electrode for recording DC potential changes accompanying spreading depression in the freely moving rat", Physiology & Behavior, 18, pp. 1171-1174, 1977.

[Shinwari 2006] Shinwari, M. W., et al., "Study of the electrolyte-insulator-semiconductor field-effect transistor (EISFET) with applications in biosensor design", Microelectronics Reliability, 47, 2025-2057, 2006.

[Shinwari 2007] Shinwari, M. W., et al., "Modeling and simulation of electrochemical DNA biosensors in CMOS technology", M.Sc. thesis, McMaster University, 2007.

[Shinwari 2008] Shinwari, M. W., et al., "Analytic modelling of biotransistors", IET Circuits Devices Systems, 2, pp. 158-165, 2008.

[Shinwari 2010] Shinwari, M. W., et al., "Microfabricated reference electrodes and their biosensing applications", Sensors, 10, pp. 1679-1715, 2010.

[Simonis 2001] Simonis, A., et al., "A "hybrid" thin-film pH sensor with integrated thick-film reference", Sensors, 1, pp. 183-192, 2001.

[Simonis 2004] Simonis, A., et al., "New concepts of miniaturised reference electrodes in silicon technology for potentiometric sensor systems", Sensors and Actuators B, 103, pp. 429-435, 2004.

[Simonis 2005] Simonis, A., et al., "Miniaturised reference electrodes for field-effect sensors compatible to silicon chip technology", Electrochimica Acta, 51, pp. 930-937, 2005.

[Sinsabaugh 1986] Sinsabaugh, S. L., et al., "A batch-processed reference micro electrode integrated on a silicon substrate", Proceeding of the Electrochemical Society, 86, pp. 66-73, 1986.

[Smith 1984] Smith, R. L., et al., "A solid state miniature reference electrode," in: Proceedings of the IEEE/VSF Symposium on Biosensors, Los Angeles, CA, pp. 61-62, September 1984.

[Smith 1986] Smith, R. L., et al., "An integrated sensor for electrochemical measurements", IEEE Transactions on Biomedical Engineering, BME-33, pp. 82-90, 1986.

[Smith 1986] Smith, R. L., et al., "Miniature liquid junction reference electrode and an integrated solid state electrochemical sensor including the same", US patent 4592824, 1986.

[Stryer 1995] Stryer, L., "Biochemistry", 4th edition, W.H. Freeman and Company, 1995.

[Sun 2006] Sun, X., et al., "Fabrication and characterization of planar reference electrode for on-chip electroanalysis", Electrochimica Acta, 52, pp. 427-433, 2006.

[Suzuki 1998] Suzuki, H., et al., "Problems associated with the thin-film Ag/AgCl reference electrode and a novel structure with improved durability", Sensors & Actuators B, 46, pp. 104-113, 1998.

[Suzuki 1998] Suzuki, H., et al., "Micromachined liquid-junction Ag/AgCl reference electrode", Sensors and Actuators B, 46, pp. 146-154, 1998.

[Suzuki 1999] Suzuki, H., et al., "Microfabricated liquid junction Ag/AgCl reference electrode and its application to a one-chip potentiometric sensor", Analytical Chemistry, 71, pp. 5069-5075, 1999.

[Suzuki 2000] Suzuki, H., "Advances in microfabrication of electrochemical sensors and systems", Electroanalysis, 12, pp. 703-715, 2000.

[Thomas 1981] Thomas, R. C., et al., "A liquid ion-exchanger alternative to KCl for filling intracellular reference microelectrodes," Pflügers Archiv European Journal of Physiology, 390, pp. 96-98, 1981.

[Tymecki 2004] Tymecki, L., "Screen-printed reference electrodes for potentiometric measurements", Analytica Chimica Acta, 526, pp. 3-11, 2004.

[Valdés-Ramírez 2005] Valdés-Ramírez, G. et al., "Composites: a novel alternative to construct solid-state Ag/AgCl reference electrodes", Sensors and Actuators B, 110, pp. 264-270, 2005.

[Van den Berg 1990] Van den Berg, A., et al., "A micro-volume open liquid-junction reference electrode for pH-ISFETs", Sensors and Actuators B, 1, pp. 425-432, 1990.

[Vasile 1965] Vasile, M. J., et al., "The preparation and thermodynamic properties of a palladium-hydrogen electrode", Electrochemical Society, 112, pp. 864-870, 1965.

[Wang 2002] Wang, M., et al., "A long-term stable iridium oxide pH electrode", Sensors and Actuators B, 81, pp. 313-315, 2002.

[Will 1986] Will, F. G., "A self-contained miniature hydrogen reference electrode", Electrochemical Society, 133, pp. 454-455, 1986.

[Wilson 2001] Wilson, D. M., et al., "Chemical sensors for portable, handheld instruments", IEEE Sensors Journal, 1, pp. 256-274, December 2001.

[Wolfe 2005] Wolfe R. C., et al., "Measurement of pH gradients in the crevice corrosion of iron using a palladium hydride microelectrode", Electrochemical Society, 152, pp. B82-B88, 2005.

[Wong 1988] Wong, H., et al., "A CMOS-Integrated ISFET-Operational amplifier chemical sensor employing differential sensing", IEEE Transactions on Electron Devices, 36, pp. 479-487, 1989.

[World Health Organization Report 2009] "Global health risks: mortality and burden of disease attributable to selected major risks", WHO press, 2009.

[Wu 2005] Wu, H., et al., "Construction of microfluidic chips using polydimethylsiloxane for adhesive bonding", Lab On a Chip, 5, pp. 1393-1398, 2005.

[Yalcinkaya 1997] Yalcinkaya, F., et al., "Ag/AgCl/Cl^- coated silver stripe reference electrode", Medical Engineering and Physics, 19, pp. 299-301, 1997.

[Yang 2004] Yang, H., et al, "An iridium oxide reference electrode for use in microfabricated biosensors and biochips", Lab on a Chip, 4, pp. 42-46, 2004.

[Yee 1988] Yee, S., et al., "Miniature liquid junction reference electrode with micromachined silicon cavity", Sensors and Actuators, 15, pp. 337-345, 1988.

[Yosypchuk 2003] Yosypchuk, B., et al., "Reference electrodes based on solid amalgams", Electroanalysis, 16, pp. 238-241, 2003.

[Yun 2000] Yun, K-S., et al., "Analysis of heavy-metal ions using mercury microelectrodes and a solid-state reference electrode on a Si wafer," Japanese Journal of Applied Physics, 39, pp. 7159-7163, 2000.

[Zhang 1996] Zhang, X., et al., "Over-oxidized polypyrrole-modified carbon fibre ultramicroelectrode with an integrated silver/silver chloride reference electrode for the selective voltammetric measurement of dopamine in extremely small sample volumes," Analyst, 121, pp. 1817-1822, 1996.

[Zhang 1999] Zhang, X., et al., "Glucose nanosensor based on prussian-blue modified carbon-fiber cone nanoelectrode and an integrated reference electrode", Electroanalysis, 11, pp. 944-949, 1999.

[Zielińska 2002] Zielińska, R., et al., "All-solid-state planar miniature ion-selective chloride electrode," Analytical Chimica Acta, 451, pp. 243-249, 2002.

Appendix 1

Bare Silver/Silver Chloride Fabrication

1. Obtain a silver wire with length of ~5cm.
2. Rinse the silver wire with acetone followed by DI water.
3. Rinse the silver wire with dilute HCl followed by DI water.
4. Prepare 1 M KCl solution by dissolving proper amount of KCl powder in DI water.
5. Dip 1 cm of the silver wire and 1 cm of a platinum wire in KCl solution with 1 cm spacing using a laboratory clamp.
6. Obtain the appropriate power supply (AC or DC) and connect its anode to the silver and its cathode to the platinum wire.
7. Apply the pre-defined potential for 15 minutes.

Appendix 2

Master Mold Fabrication

8. Dip the Si wafer in Acetone followed by Methanol for 20 seconds for each step.
9. Rinse the wafer by running DI water for 5 minutes.
10. Place the wafer on hot plate at 110 C for 2 minutes.
11. Place the wafer in oxygen plasma at 50 Watt exposure for 1 minute.
12. Spin Su-8-100 photoresist on the wafer at 500 rpm for 30 seconds.
13. Ramp the speed up to 1700 rpm in 6 sec and continue spinning for 40 sec at this speed.
14. Prebake the wafer for 12 minutes at 65 C.
15. Increase the temperature 10 degrees per minute up to 95 C.
16. Bake it at the final temperature for 1 hour.
17. Mount the mask and the wafer on mask aligner and align them together.
18. Expose the wafer to UV light with power of 6.8-mWatt for 95 seconds.
19. Post-bake the wafer at 65 C for 5 minutes.
20. Increase the temperature 10 C per minute up to 95C.
21. Bake the wafer at the final temperature for 10 minutes.
22. Develop the wafer by developer until features with shape of the microchannel appear on the wafer (about 30 minute).
23. Rinse the wafer with IPA to ensure complete removal of unexposed Su-8.
24. If IPA leaves white residues on the wafer, the developing process should be repeated.

Appendix 3

Device Assembly Process

1. Obtain PDMS pre-polymer by mixing thoroughly 20 mL of base and 2 mL of curing agent.
2. Place the fabricated mold on a plastic Petri-dish covered by an Aluminum foil.
3. Pour PDMS pre-polymer on the mold and place it inside a vacuum pump until the bubbles inside the bulk PDMS disappears.
4. Place the wafer on hot plate at 80°C for 2 hour.
5. Clean top surface of the microchannels in oxygen plasma at 50 Watts for 1 min.
6. Obtain a PDMS pre-polymer by mixing 1 mL base and 3 mL curing agent.
7. Spin a droplet of prepared PDMS pre-polymer on a silicon wafer at 500 rpm.
8. Ramp the spinning speed by 1000 rpm/sec up to 10000 rpm.
9. Continue spinning at the final speed for 4 minutes.
10. Place the microchannel facedown on the obtained thin uniform PDMS pre-polymer.
11. Ensure there is no gap between the adhesive pre-polymer and the top surface.
12. Lift off the microchannel carefully.
13. Penetrate a 18 ½ gauge needle in microchannel reservoir.
14. Pass the fabricated Ag/AgCl wire through the needle into the reservoir until approximately 1 mm of the AgCl region comes out of the needle.
15. Laminate the polycarbonate membrane on the microchannel top surface.
16. Use another PDMS microchannel as a microcontact printing stamp.

17. Place it facedown on the thin PDMS pre-polymer layer.
18. Align it perpendicularly with the underlying microchannel to print the PDMS pre-polymer on the membrane.
19. Obtain a PDMS top layer (2 cm wide, 5 cm long, 1 mm thick) with a central opening and two through holes (1.2 mm in diameter) at the endings.
20. Bond it onto the membrane using the microcontact printing to enclose the microchannel.
21. Cure the device at 80°C for 4 hours.
22. Obtain two PDMS blocks (1 cm wide, 1 cm long, 5 mm thick) with central holes (1.2 mm diameter).
23. Attach interconnections (plastic tubes with inner diameter of 0.8 mm and outer diameter of 1.2 mm) in punched area of the PDMS blocks.
24. Assemble the PDMS blocks onto the PDMS top layer of the device by the PDMS pre-polymer.
25. Cure the assembled device at 80 C° for 2 hours on hotplate.
26. Shield the electrode (the part left out of the device) by a plastic tube (inner diameter of 1.6 mm) and PDMS pre-polymer at connection area.
27. Cure the device at 80°C for 2 hours on hotplate.